BSPE 00325-558-5

해상 Gradiometer 자료의 처리 및 해석기법에 관한 연구

Study on Processing and Interpretation of Marine Gradiometer Data

1993. 3.

한 국 해 양 연 구 소

제 출 문

한국해양연구소장 귀하

본 보고서를 " 해상 Gradiometer 자료의 처리 및 해석기법에 관한 연구" 과제의 최종보고서로 제출합니다.

1993년 5월

연 구 책 임 자 : 박 찬 홍
연 구 원 : 박 건 태
정 백 훈
장 계 경
연 구 조 원 : 주 용

요 약 문

I. 제 목

해상 Gradiometer 자료의 처리 및 해석기법에 관한 연구

II. 연구개발의 목적 및 중요성

일반적으로 해상에서 측정되는 지자장에는 지하지질구조에서 유발되는 자기이상뿐만 아니라 시간에 따라 주기적 혹은 비주기적으로 발생되는 자기장을 포함한다. 이와 같은 시간에 따른 자기장의 변화는 주로 태양의 흑점활동이나 태양풍(solar wind)의 작용으로 지구외부의 자기권에 영향을 줌으로써 발생된다.

지금까지 국내에서는 해상과 조사해역에서 가까운 해안 지역에 고정 관측소에서 동시적으로 측정하여 시간적 변화량을 소거하는 방법을 사용하였다. 그러나 이와 같은 방법은 언제나 시간적,인적,경제적 비용을 수반할 뿐만 아니라 일명 'coastal effects'로 불리는 대륙지각과 해양지각의 경계부에서 발생하는 불규칙한 자기장을 포함하기 때문에 시간적 변화를 완전히 분리는 것이 어렵다.

Gradiometer에 의한 지자기 측정은 감지기의 방향에 관계없이 지자기의 시간적 변화량을 자동적으로 보정할 수 있어서 통상적으로 지자기 일변화 보정을 위한 고정관측소를 별도로 운영하지 않으면 안되는 원해지역, 지자기 활동이 극

히 활발한 극지,적도지방 뿐만아니라 육지의 자력원으로부터 많은 유도자기를 포함하는 해안지역에서도 해상측정만으로 시간적 변화가 보정된 정밀한 자력치를 얻을 수 있을 있다. 그러므로 gradiometer 자료는 정밀한 자기이상의 변화의 분석이 필요한 해저송유관,해저전력선,침몰선체로부터 유발되는 신호를 보다 정확하고 용이하게 인식할 수 있도록 해줄 뿐만 아니라 현재 본소에서 수행중인 해역방위 연구사업이나 최근 도입 운영중에 있는 다중채널 탄성파 탐사로 부터 얻는 심부 지질구조와의 비교해석 및 대륙붕 자원 탐사,심해저 망간단괴 개발사업에서 지하지질 구조 해석이나 지자기의 시간적 변화 특성 분석 및 해양지각의 확장 역사등의 해석에 매우 유용하게 활용될 수 있다.

본 연구에서는 해양 조사선 이어도에 설치된 gradiometer의 현장 운용을 통해 자료 획득시스템을 구축하고 처리 소프트웨어 운용기술을 습득하여 향후 gradiometer의 원활한 운용의 기반을 마련하고 실자료의 처리 결과를 조사해역내 해저에 설치된 OBEM에 의해서 장기간 관측된 지자기 일변화 자료와 비교 검토함으로써 신뢰도를 검증하고 보정된 자기이상치로써 지하지질구조와를 해석하는 데 주요 목적이 있다.

III. 연구개발의 내용 및 범위

Gradiometer를 이용한 측정자료의 실시간 디지탈 입출력 시스템 ,기본적 현장 자료처리등을 포함하는 현장 운용기술과 측정에서 발생되는 잡음(noise) 특성 파악하고 이를 제거하는 방법을 제시한다. 또한 MGS S/W를 이용하여 실자료를 처리함으로써 지자기의 시간변화가 보정된 순수한 지하 지질구조에 의한 자기장만을 분리하고 OBEM 자료와 비교 검토함으로써 신뢰도를 검증하고 지하지질구조와

관계를 규명하였으며 연구내용 및 범위는 다음과 같다.

(1) Gradiometer 현장 운용시험 및 체제 확립

(2) 현장 측정자료의 실시간 디지탈 입출력 시스템 및 단순 자료처리 기술 개발

(3) 조사선 이어도를 이용한 동해 일원 현장 관측

(4) MGS(Marine Gradiometer Software)를 이용한 자료처리 및 문제점 검토

(5) OBEM(해저지자기측정기)의 지자기 시간적 변화와 비교를 통한 신뢰도 검증

(6) 자기이상치의 지질구조와 상관관계 해석

IV. 연구개발 결과 및 활용에 대한 건의

본 연구에서 얻은 결과는 다음과 같이 요약된다.

(1) 동해 일원의 현장탐사를 통해서 국내 최초의 gradiometer system의 실시간 디지탈 입출력 시스템의 완성을 비롯한 현장 운용 기술 및 자료처리 기술의 기반을 확립하였다.

(2) 조사선 선체로부터의 간섭되는 자기장의 특성을 파악할수 있었으며 이를 효과적으로 제거하였다.

(3) 선체의 주항 방향에 따른 선행 감지기에 미치는 조사선 선체의 영향은 3 내지 4 nT였다.

(4) Gradiometer 자료에 의한 지자장 일변화의 소거 목적으로 gradient의 적분 방법 및 optimum filter 방법등 두 가지 방법이 적용되었으며, optimum filter 적용 결과 적분 방법에 비해서 성공적으로 지자장의 일변화를 분리할 수 있었다.

(5) Gradiometer에 의해 산출된 지자장 일변화는 OBEM 측정 결과와 비교적 잘 일치하였다.

(6) 측선 6 과 측선 8의 일부구간에서 gradiometer로 부터 계산된 자기장의 시간적 변화는 -35 nT에서 40 nT로써 매우 크며 그 변화 양상도 매우 불규칙 하여 지자장이 교란되었음을 지시한다.

Gradiometer의 활용이 가능해짐으로써 육상고정관측소 운영에 따른 경제적, 인적 비용을 절감할 수 있게 되었으며 조사해역의 원근 및 위도에 관계없이 지자기의 시간적 변화에 무관한 자기이상치의 산출이 가능하게 되었다. 연구결과는 해역방위 연구나 해저자원 개발 및 지구조연구등의 목적에 매우 유용하게 활용될 수 있다. 특히 본소에서 현장자료 획득 및 처리에 성공한 다중채널 탄성파 자료, OBS(Ocean Bottom Seismometer) 자료 및 중력자료와의 통합해석을 통한 보다 정확한 심부지각구조 연구가 가능해지며 해양지각의 연대측정에 중요한 단서를 제공할 것이다.

CONTENTS

LIST of FIGURES

1. INTRODUCTION

Measurements of the earth's magnetic field inherently include unpredictable time dependent vatiations with a relatively short period of several hours,minutes or seconds. Time variations of the earth's magnetic field in magnetic survey could result in serious misinterpretation for geological structure without its suppressions. For that reason how to separate the time variation from magnetic observations for the purpose of subsurface geological studies has been dealt with as a considerably highlighted problem with a number of techniques.

In earlier stage the time variations were corrected by eliminating a long range wavelength function led from statistical approaches with cross over differences at many tie points from the data. This method may be valid where many survey tracks are regularly spaced and the time variations change slowly. However if the period of the time variations were shorter than the time interval between the crossings,the correction will not either be made, or cause aliasing. Moreover because survey tracks at marine are often likely to be open spaced, irregular, or only a few, this method in such a case can not complete an adquate correction of time variation.

As the second methed onshore magnetic base stations near the survey area have been used for measuring the earth's magnetic field and removing the time variations. However, the temporal variations of the earth's magnetic field can produce large differences in its phase and amplitude changes at far distances. Moreover the magnetic measurements near near onshore are usually influenced by the Coastal Effect which pertains to the anomalous behavior of micropusations resulting from the differences in electrical conductivity between the continental and the oceanic crust. These conductivity differences give rise to the induction of currents by magnetosphere in the subsurface that are substantially different within the coastal shore and within

the vicinity just onshore and near this interface. Therefore discordances inevitably exist in between the time variation measured at onshore base station and offshore at a distance of over tens kilometers using magnetometer. Better measurements can be accomplished by using the Ocean Bottom Magentometer in marine survey area. However such a method is impractical in normal survey because it requires special devices, much time, and more expences.

Marine gradiometer can even more enhance a resolution of magnetic anomalies for interpreting subsurface sources by suppressing time variations of the earth's field including even magneitic storm with easy acquisition and relatively simple analysis method. The differential between the sensors is free of time variation including magnetic storms, diurnal variations, and micropulsations because the time variation will be simultaneously measured with almost the same values. Wold and Cooper(1987) illustrated how marine magnetic gradiometer data can effectively give better magnetic information about geological structures in interpreting seismic data by combining gradiometer data and seismic sections.

This study will firstly review the principle of the gradiometric method, set up the acquisition system of the marine gradiometer(G811G, E&G Geometrics) installed in the R/V EARDO(350 tonnage) and complete how to properly deal with it through a field test. Also various corrections for the gradiometer data and reconstruction process of magnetic field free of time variations will be studied and its validities will be discussed by comparing the result with magnetic observations from OBEM established on the seabottom in the survey area.

2. PRINCIPLES OF GRADIOMETRIC METHOD

When total magnetic intensities are measured simultaneously from two total magnetic sensors at distance between each other on a singe line, the same time variations in both sensor will be detected and the time variation can be separated through simple analysis.

The forward sensor is at a sufficient distance from the ship to minimize the effects of the ship's magnetic field, generally three times of ship's length. The rear sensor is trailed at a distance behind the forward one so that the difference between the observed fields in both could be dominated by the geological differences rather than noises, but close enough that the difference could be used to approximate the geological gradient.

In convensional method to reconstruct the time variation free magenetic field used numerical integration of the gradient which is the differences between two sensors divided by the distance. However, it is usually difficault to produce a satisfactory result because different kinds of noises are amplifed in the process of calculating the gradient and re-intergrating it.

An alternative approach has been developed to minimize the effects of these errors and to suppress the time variation by Hansen(1984). This method , based on optimum filter theory, was developed to minimize the effects of these errors producing in the process of forming the gradient and intergrating it to reconstruct the magnetic field free of the time variation. Both the slave and mster sensor data are Fourier transformed using the routine DFT, and the responce function for the reconstruction filter at each frequency is then computed and apllied to the data set. After reconstruction, the output data are inverse Fourier transformed and the average linear trend from the input data are added in order to achieve reasonable ranges for the output.

3. GRADIOMETER MEASUREMENT ERRORS

Gradiometer measurements are affected by mainly four classes error sources: system noise, for examples, instrument noise and electrical interference; heading error; geometrical effect; and wave noise and sensor motion.

3-1. System Noise

For Model G811g gradiometer used in our survey because the instrument noise which refers to accuracy is as small as 0.01 nT,instrument noise levels can be expected to appear as an irreducible source of white noise at a fixed level in data set. Electrical interference also shows up as white noise level even if it is normally much larger than the instrument noise.

3-2. Heading Error

Heading errors are mainly arised from the ship's permanent field and the induced field caused by the interaction of the earth's field with the magnetically permeable materials in the ship. According to Bullard and Marson(1961) the heading error will be estimated as the below descriptions.

The permanent field of the ship at a location fixed with respect to the ship may be resolved into 3 components of a tranverse component Y, a longitudinal component X, and a vertical component V. If the magnetic heading is ζ, and the inclination of the earth's field is θ, then the strength of the permanent field will be

$$H_p = Y\cos\theta \sin\zeta + X \cos\theta \cos\zeta + V \sin\theta \qquad (2\text{-}1)$$

As to each components of the earth's field the secondary magnetic fields will be induced dependent on the ship's magnetic properties and added to the measurements in a magnetic sensor as much as

$$\begin{aligned} H_i = H_e(&YY\cos^2\theta \sin^2\zeta + YX \cos^2\theta \sin\zeta \cos^2\zeta + YV \sin\theta \cos\theta \sin\zeta \\ &+ XY\cos^2\theta \sin\zeta \cos\zeta + XX \cos^2\theta \cos^2\zeta + XV \sin\theta \cos\theta \cos\zeta \\ &+ VY\sin\theta \cos\theta \sin\zeta + VX\sin\theta \cos\theta \cos\zeta + VV\sin^2\theta) \end{aligned} \qquad (2\text{-}2)$$

However, because the earth's field intensity H_e and the inclination may be regarded as constants in the normal survey whose area is not quite large, those terms could be ignored and led to result in the following empirical expression

$$H_s = A + B \sin\zeta + C \cos\zeta + D \sin 2\zeta + E \cos 2\zeta$$

Where, the coefficients A,B,C,D, and E depend not only on the permanent and induced effect but also on the intensity and the inclination of the earth's magnetic field. But because the coefficients A,B,C,D, and E may be treated as constants for a reasonable area, only the ship's magnetic heading is a variable

in the final expression.

3-3. Geometrical Error

A simplified tow system is given to analyze the geometrical effects of tow sensors with respect to the ship on a plane as Fig. 1. If V is the ship's speed over land, then the speed through the water is Vw = V - Vc and it is also the tow system's speed because the system lies in steady state. The ship exerts a tension T on the tow system along the tow system axis. Since the entire system is in the steady state, this is exactly balanced by the drag of the tow system through the water. Thus the tow angle ψ' is determined by the force balance. Let the coefficient of draft be σL along the tow system axis, and σT perpendicular to the axis.

This simplifies the calculation of the heading errors, as the entire system can be treated as a rigid body. However on the other hand heading errors can be changeable along the track due to current conditions.

The tow system in the vertical profile can be represented as Fig. 2. The assumtions given to this system are that the system is in the steady state, that the the tow system can be treated as a lumped mass on a resistanceless, massless string, and that the drag follows the Stock's law. If let γ the dip angle of the tow system, δV the coefficient of drag in the upward vertical direction,.and m the mass of the tow system, then resolutions of forces along and perpendicular the tow system can be expressed as

$$T = \sigma L\, V_w \cos\gamma + mg \sin\gamma$$
$$\sigma V\, V_w \sin\gamma = mg \cos\gamma$$

From the second equation, it follows that the dip angle is given by

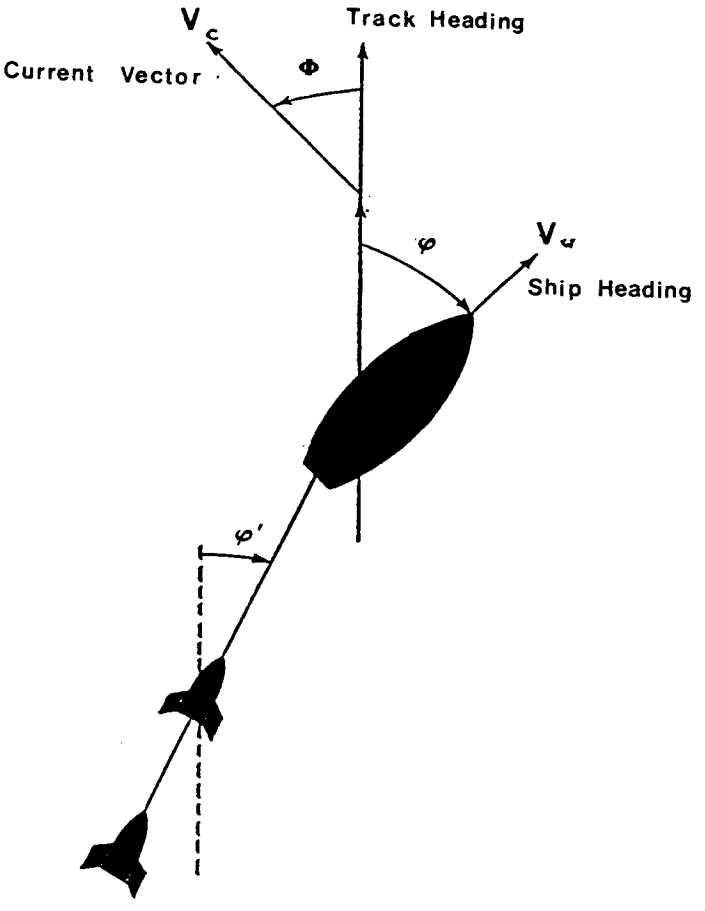

Fig. 1. Geometry of the tow system

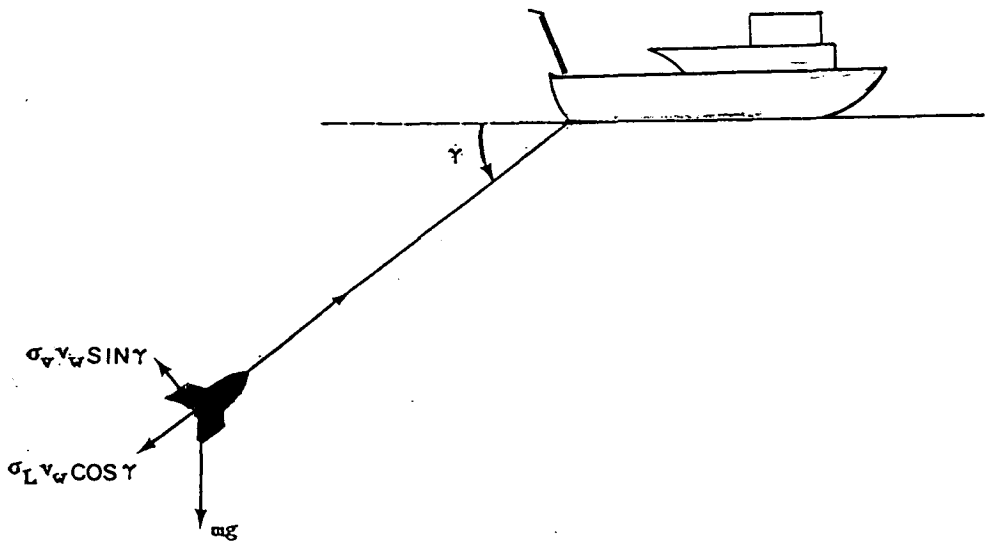

Fig. 2. The vertical profile of the tow system

$$\tan\gamma = \frac{mg}{V}\frac{1}{V_w}$$

The errors which arise from the geometry of the system can be described as three cases. Firstly, the cross currents and the dip of the tow system always make the lag between the sensors along the track heading remain smaller than the actual distance along the cable. Secondly, since the rear sensor is always trailed in deeper depth than the forward sensor, the magenic fields downward-continued as much as its gap will be measuerd in the trailing sensor. Finally owing to the leeway the trailing sensor will be displaced horizontally on the track. Tow system should be well-designed to minimize these geometrical errors in every survey.

3-4. Swell Noise and Sensor Motion

Sea swell noise is caused by a periodic motion of sea water in the earth's magnetic field . Swell noise appears as a periodic variation of a few nT at the periodic wave motion of 10 to 20 sec(Hansen,1985). However because according to the test result with the sampling rates of the same order as the wave motion period of 4 to 10 seconds the wave noise was not identifiable in any records, in practice wave correction will be required only for high resolution and rapid sampled magnetic data. Because errors due to hydrodynamic instabilities of the tow system remain in relatively smaller order, it can be likely negligible if tow system is well designed and sensor motion does not highly exceed a normal state.

4. ERROR ANALYSIS

Because error effects in reconstructing the total field anomaly by intergrating its gradient may result in amplifying, they are required to remove as much as if possible before reconstruction processing.

The slave and master signals can be expressed in time dependence as

$$m_1(t) = \gamma(t-\frac{\tau}{2})+d(t)+n_1(t)$$

and

$$m_2(t) = \gamma(t-\frac{\tau}{2})+d(t)+n_2(t)$$

respectively, where $\gamma(t)$ is the geological signal, $d(t)$ the time variation, $n_1(t)$ and $n_2(t)$ the errors in the two sensors, and τ is the sensor lag in time. The gradient from two sensor signals is

$$\frac{1}{\tau}\delta_m(t) = \frac{1}{\tau}((\gamma+\frac{\tau}{2})-(\gamma-\frac{\tau}{2}))+\frac{1}{\tau}\delta_n(t)$$

and Fourier transformation for that comes

$$\frac{1}{\tau}\delta M(\omega) = \frac{1}{\tau}(e^{i\frac{\omega\tau}{2}}-e^{-i\frac{\omega\tau}{2}})G(\omega)+\frac{1}{\tau}\delta N(\omega) \qquad (4\text{-}1)$$

Applying the Fourier transformed integration operator, $I(\omega) = 1/i\omega$ give

$$\frac{1}{\tau} I(\omega)\delta M(\omega) = \frac{e^{\frac{i\omega\tau}{2}} - e^{\frac{-i\omega\tau}{2}}}{i\omega\tau} G(\omega) + \frac{1}{i\omega\tau}\delta N(\omega)$$

Because at low frequencies

$$e^{i\frac{\omega\tau}{2}} - e^{-i\frac{\omega\tau}{2}} \cong i\omega\tau$$

holds, so the term mutiplying G(ω) on the right-hand side of Eq.(4-1) is unity. Thus, the integration operator correctly reconstructs the low-frequency behavior of the geology signal. The operator actually vanishes for $\omega\tau = \pi$, which reflects the fact that for finite sensor separations the difference is only an approximation to the gradient. If the accurate reconstruction of the signal at those frequencies is required, a sensor separation must be smaller.

The effect of leeway and vertical separation of the sensors on the sensor lag along the track will lead to a sensor separation shorter than the cable distance between them. Thus if the cable distance L is divided by the speed V to give a lag τ' which is used to divided the sensor difference, τ' will be given by

$$\tau' = \tau + \delta\tau,$$

where $\delta\tau$ is in general positive. The ratio multiplying G(ω) in Eq.(4-1) will then be

$$\frac{e^{i\frac{\omega\tau}{2}} - e^{-i\frac{\omega\tau}{2}}}{\tau + \delta\tau}$$

which will lead to underestimation of the variation in the geology signal by factor

$$\frac{1}{1+\frac{\delta\tau}{\tau}}$$

at all frequencies. The effect of accepting the obvious value for the lag estimates is therefore to reduce the amplitude of all geological anomalies by this factor.

Consider next the effect of the vertical separation between sensors. If the vertical separation is z, and if the geology is approximately two-dimensional, then the Fourier transformm of the geology signal at the trailing sensor is modified by the factor

$$e^{\frac{|\omega|\delta z}{v}}$$

Thus the error term in this case can be written

$$N(\omega) = (e^{\frac{|\omega|\delta z}{v}} - 1)e^{-i\frac{\omega\tau}{2}} G(\omega)$$

Since this expression vanishes as $0(\omega)$ at DC, the effects of an error term of this type are bounded at low frequency, even when multiplied by a factor $1/\omega$. At high frequencies, the effects are more important; but in this limit the multiplication by $1/\omega$ tends to damp the errors. Thus, except for rather large values of δz (of the order of the distance to the geologic sources), one expects the effects of the differential in tow depth to be unimportant.

As for the wave noise and sensor instability errors, the dominant effects are periodic with periods not much larger than the sampling rate. The effects of these errors will therefore be minimal, as the integration causes the errors to be multiplied by $1/\omega$.

The rest of errors will be introduced by the system noise, the heading errors, and the spatial mislocation effects. System noise, being approximately white, has a roughly flat spectrum and so will be amplified at low frequency by integration. However, it is reasonable to hope that the overal level of system noise is quite low. Heading errors are predominantly a low-frequency phenomenan, and so may be expected to cause very serious problems unless the wavelengths are longer than the line length. That is,to the extent that heading errors are not exactly constant along the line, very large errors in the re-integrated field can be expected.

Finally, the spatial mislocation effects depend on the behavior of the geology transverse to the line direction. To the extent that the geology is exactly two-dimensional, these errors are harmless. The deviations from two-dimensionality will also tend to have rather long wavelengths, so the resulting errors can be expected to produce serious effects in the integrated gradient.

5. RECONSTRUCTION OF TOTAL FIELD

5-1. Integration Method

The time varying effects can be cleared through common mode rejection method by calculating the differences between measurements from two

sensors. The difference of the total field intensities devided by the fixed distance between the sensors is the gradient of the total field. The differential magnetic fields consist of the more subtle local anomalies free of large anomalies that originate from deep geological sources. Integrating the gradient along the path produces a total magnetic field free of time variations. The constant of integration is merely the intensity at one sensor and can be used to refer the integrated gradient to prevent large cumulative integration errors.

The gradient can be written by

$$\frac{dT}{dx} = \lim_{\Delta x \to 0} \frac{T_x - T_{x+\Delta x}}{\Delta x} \approx \frac{\Delta T}{\Delta x}$$

where $\Delta T = T_x - T_{x+\Delta x}$ is difference of total intensities between the two sensors, ΔX the distance between sensors, and $\frac{dT}{dX}$ the gradient expressed as the derivative in the direction of the traverse. The $\Delta X \to 0$ indicates that this expression is valid when ΔX approaches zero, i.e., if ΔX is small with respect to the distance to the nearest sources of magnetic anomalies. In practice, the sensor spacing, ΔX, should be smaller than one-fifth the distance to the nearest sources. If such conditions are satisfied, $\frac{dT}{dX} = \frac{\Delta T}{\Delta X}$ is the gradient along the direction of the traverse. The longitudinal gradient is integrated along the traverse(x-direction) over an integration distance conveniently selected to be long enough to reduce short period noise and yet be short enough to be sure that this distance is a small fraction of the typical anomaly wavelength. The measured gradients will be integrated over ΔX as

$$\int_{x_0}^{x_1} \frac{dT}{dX} \Delta x = T_i + F_0$$

where F_0 is the constant of integration, which in this case is simply the total intensity observed at the rear sensor at the starting point of the integrating procedures. T_i is the incremental total field obtained by integration and is free of time variations.

4-2. Fourier Transform Method

The final approach of gradiometric method is to get the diurnal free magnetic field of the earth's fields from the observed signals. The total magnetic fields measured in two sensors of gradiometer include several kinds of components of such as the ship's influence,the earth's diurnal variations,noises,and so on as well as the geological sources. The observed magnetic fields at each sensor can be represented as

$$f_1(t) = m(s) + d(s,t) + h_1(t) + b_1(t) + n_1(t)$$

$$f_2(t) = w(z)m(s-\Delta s) + d(s,t) + h_2(t) + b_2(t) + n_2(t)$$

where

$f_1(t)$ is the observed field at the forward sensor

$f_2(t)$ is the observed field at the rear sensor

$m(s)$ is the diurnal free earth's field

$d(s,t)$ is the diurnal field

$h_1(t)$ and $h_2(t)$ are the ship's effects

$b_1(t)$ and $b_2(t)$ are biases fields arised from magnetic effects local to each sensor

$n_1(t)$ and $n_2(t)$ are noises due to electronical interference,sea water action, and so on

Δs is the horizontal separation between the sensors

$w(z)$ is the downward continuation operator for vertical sensor separation

and s means time dependent distance ,that is, $s(t)$.

If the following assumptions are properly satisfied to the terms of the observed field , a unique field can be reduced. However practically it inevitably includes errors.

As the first assumtion the ship's field depends only on the ship's heading. It can lead to model the ship's magnetic effect with a simple geometrical scheme as the method used by Bullard and Mason(1961). This assumption can be fairly applied to the case in which the earth's field is

almost constant over the survey area, the ship's speed maintains approximately constant,and systemetic misalignment of the sensors is negligible. However a more complicated model should be constructed if the ship's speed changes very much and the survey is excuted over a broad area.

Secondly the biases b_1 and b_2 is assumed to be constants. It means that the magnetic effects from sources near the sensor may be independent on position, speed, or heading.

Thirdly the ship's speed, and the horizontal and vertical separation between the sensors, are approximately constant over distances comparable to the sensor separation, except for random components whose effects may be included in n_1 and n_2.

Fourthly the gradient of the earth's field transverse to the profile is small enough that upward continuation of the field can be performed on profile data alone.

The last assumes that the noise terms n_1 and n_2 are approximately white, zero-mean, and random time series.

The reconstruction of magnetic fields free of time variation from the observed begins with a removal of the ship's field by estimating a set of coefficients in Eq.(2-3). The coefficients can be obtained from line by line data set itself in case of low level survey as well as sufficiently large data sets over almost all of the lines. Magnetic fields resulted from a set of coefficients will be removed from the observed data, which will be resulted in corrected magnetic fields f_1',and f_2'. The difference between those two fields is

$$f'(t) = f_1'(t) - f_2'(t)$$

$$= m(s(t)) - w(z)m(s - \Delta s) + \Delta b + \Delta n(t)$$

This expression will be Fourier-transformed in space along the ship's track by choosing such that Δs and Δz are approximately constant over the segment, but long enough to retain adequate frequency resolution. Then the Fourier transformed one can be denoted as

$$\Delta F'(\xi) = M(\xi) - \exp(2\pi|\xi|\Delta z)\exp(2\pi i\xi\Delta s)M(\xi) + \Delta B + \Delta N(\xi)$$

Since Δb is a constant, ΔB is zero except at $\xi=0$; on the other hand, the two terms involving $M(\xi)$ cancel at $\xi=0$, and $\Delta N(0)$ vanishes by the assupmtion that the noise terms are zero-mean time series. Thus, by subtracting a constant from $\Delta f'$ to make its mean to be zero, the bias difference may be removed from the entire data set, so that

$$\Delta F''(\xi) = M(\xi) - \exp(2\pi|\xi|\Delta z)\exp(2\pi i\xi\Delta s)M(\xi) + \Delta N(\xi)$$

holds.

A smoothing operator will be applied to the spectrum. Since Δn is assumed to be white, while the field m should be slowly varying in frequency, this smoothing operator can be chosen so that the soothed noise term ΔN vanishes approximately. The exponential terms are also assumed to be unaffected. From the assumptions

$$\Delta F''(\xi) = M(\xi) - \exp(2\pi|\xi|\Delta z)\exp(2\pi i\xi\Delta s)M(\xi)$$

or for $\xi \neq 0$,

$$M(\xi) = \frac{\Delta F''(\xi)}{1-\exp(2\pi|\xi|\Delta z)\exp(2\pi i\xi\Delta s)}$$

are resulted in.

Thus, the filter for reconstructing the field m from the observed is the composition of a spectral smoothing operator with a filter which approximates

$$\frac{1}{1-\exp(2\pi|\xi|\Delta z)\exp(2\pi i\xi\Delta s)}$$

To enhance the filter in the frequency domain, a sampling interval long enough to give reasonable spectral resolution, but short enough to satisfy the requirement that Δx and Δz be approximately constant, would be used for the Fourier transform. A smoothing operator would be applied to the transform, and the result successively multiplied by the proper factor. The field free of noises and diurnal effects would be reconstructed by the inverse Fourier transform.

If the term $\exp(2\pi|\xi|\Delta z)$ in the filter response is neglected, the operator required to reconstruct the field is singular at frequencies which are multiples of $1/\Delta s$. This operator must therefore be tapered to suppress the response near those frequencies. In practice, the response will be cut off completely at

$\xi = \pm \frac{1}{\Delta s}$, which limits the highest frequencies obtainable by gradiometer methods.

Next, the DC component of the field must be obtained by a separate calculation. The DC component could be interpolated from the low-frequency behavior of M. If only anomalous fields are of interest, the DC component would be completely negligible.

6. DESCRIPTION OF MGS
(Marine Gradiometer Software)

This software is used to get a unique geological magnetic effects by reconstructing of the magnetic field free from the time variation field from observed gradiometer data. The processing will be done in several ways according to data environments available as the processing flow in Fig. 3.

A brief discription on the processing flow of the software will be given as below. This software consists of seven application modules and five utility modules. Although it is recommended to excute all the application modules to get more useful results, according to user's need and processing purposes choosing items could be chageable. However the essential three steps that should be run are to convert ASCII files to MGS file(binary code), to compute logarithmic amplitude spectra, and to reconstruct fields. Derivative and simple numerical integration method can be used as a check on results from spectra method.

As a first step of the processing the observed gradiometer data set written in a ASCII from a digital recording device are converted to a binary code and formatted so as to proceed into MGS. It can work with a limit

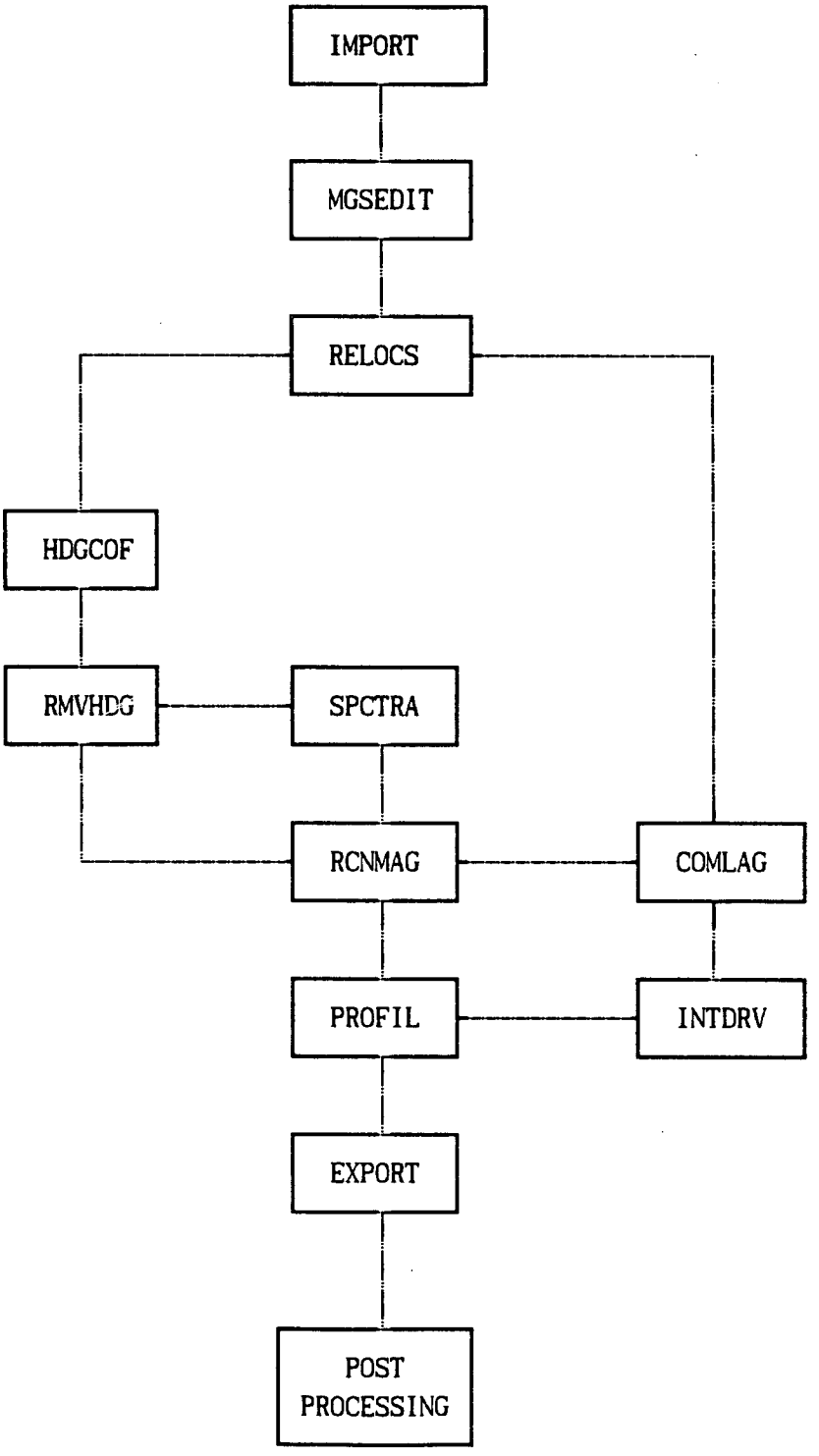

Fig. 3. Processing flow of gradiometer data

whose maximum length of one record is 255, maximum input files are eighty, and maximum number of samples allowed per lines is 5120.

The next module, RELOCS, computes the sensor midpoint locations from the ship's location, the ship's speed, and the track heading from the location and time data.

The COMLAG program computes the apparent lag between the two gradiometer sensors from a cross-correlation function. Lag is the horizontal distance between the two sensors which varies as a function of ship's speed, and computed in units of recorded samples.

The HDGCOF program computes five heading correction coefficients from the differences between two sensor readings. The output include the complete correlation matrix which could be used for diagnostic purpose. The computed coefficients will be applied to remove the heading effects of the forward(slave) sensor by the RMVHDG. For the data containing a reasonable range of heading angles(3 or 4 degrees) the least-square system is varified to be reasonably well-conditioned in actual processing. Running the HDGCOF should be avoid if only one or two dominant headings are present in the data set. Where the survey covers areas as large as the dip and intensity of the earth's field are considerably variable, the data set should be separated into blocks so that the assumptions hold. If a circled or a cloverleaf-shaped data set in a low-gradient area at or near the survey area are available, at first that data should be used in preference to the survey data itself. On the other hand if large geological gradients or time varing signals in the data set are contained, at first they must be eliminated before applying this routine. Heading angles are assumed to be positive eastward from north. If the magnetic headings are used, declination should be set to zero; otherwise use declination value proper to the survey area from the declination map.

The INTDRV program performes integration of the difference between the sensors to obtain a reconstructed magnetic field using the trapezoid rule, differentiates the master sensor fields, and computes the slave-master differences. Since unacceptable results for this reconstructed field can occur, it

is not recommended for routine geological analysis. The derivative of the master sensor is very diagnostic for detecting time variations in the data when compared with the slave-master difference. The lag values computed by the COMLAG are used to scale the sample spacing.

The SPCTRA program computes the logarithmic amplitude spectra from profile data and display the amplitue spectrum on the graphics screen or print a hard copy on the printer. This program must be run to select the parameters required in reconstruction process. Unlike the other programs in the MGS group, this program is completely interactive,prompting the user for all necessary parameters. The spectrum displayed is the Fourier transform (Singleton,1969) of the selected variable normalized in such a way that for white noise the average amplitude is equal to the RMS noise value. This is convenient for obtaining numerical estimates of noise levels directly from the logarithmic amplitude plot. The frequency units employed in the display are Nyquist units(cycles/sample), and all the interactions about scaling for the frequency axis is posed in these terms.

The RCNMAG program excutes the most important computation on reconstructing the magnetic field free of diurnal effects, and estimating the time variation fields. Both the slave and master sensor data are first prepared for the subsequent Fourier transforms. Since this step involves padding the ends of the data sets, it is very important that the input data not be excessively noisy, or the padding will generate spurious data. If very noisy data are to be used in the program, a mild low-pass filter must be applied to the data of both master and slave first. Next, both sensor's data are Fourier transformed using the same routine DFT in the SPCTRA. The response function for the reconstruction filter at each frequency is then computed and applied to the data. The filter parameters are controlled by user selected parameters. The output data from the reconstruction are inverse Fourier transformed and the average linear trend which has been removed from the input data are added in order to achieve reasonable ranges for the output. The mathematical model assumed in the program is one of decaying

exponentials for both the geology and the time variations, and white noise of equal levels for each of sensors.

Reconstruction process begins with choosing a representative sample of spectral plots from the SPCTRA program for data containing typical geology and time variation signals. While the noise dominates and appears as a flat spectrum at high frequencies, the geology is usually identifiable as one or more linear segments at low frequencies. It can be more difficult to identify the time variation signal due to possibilities to confuse it with shallow geology effects. Comparison between the slave-master difference, the derivative of the master sensor or quick depth estimates using the spectral method of Spector and Grant(1970) will be of great help in discriminating between geology and time variation field. It is important that enough amplitude spectra be examined to ensure that reasonable consistency holds for the data set. The values from the various spectra can then be averaged and used as parameters for a trial run. Each line can be separately treated tuning the parameters to get the best results locally. The noise estimate obtained from the white noise portion of the spectrum should be from the slave sensor since it is usually the noisest. Underestimating the noise may create poor results at margin,for example, the reconstructed field displaying excessive low-frequency deviation from the input profiles. This suggests increasing the value for noise until the results appear reasonable. Some edge effects are always present in the output,but not surprisingly. The edge effects are quite variable, so some judgement of the extent to which they occur must be made on a line by line basis.

7. APPLICATION TO FILED DATA

7-1. Data Aquisition

During 1992 marine gradiometric data were collected using marine gradiometer (Model G811g,EG&G) and the R/V Eardo(350 tonnage) in the Ulleung Baisn area(Fig.4). The gradiometer is equipped with two main consoles for master sensor and slave sensor respectively, 450 m tow cable and two sensors,cable winch, and data logging software(Relm,TerraSense Inc.).

Two magnetometer sensors separated by 150 m are towed behind a ship on a single tow cable. The forward sensor was as far as 200 m of more than three times of ship's length (about 50 m) behind the survey vessel to minimize the magetic field affected by the ship. Tow depths of two sensors ranged from 12 m for the slave sensor to 14 m for the master sensor with a speed of about 10 knots. Data from two sensors were sample at interval of every 1 second with 0.01 nT accuracy and recorded in personal computer using logging software.

7-2. Data Analysis and Discussion

Observed gradiometer data of 1 second interval is incorperated to GPS positioning data and reformatted so that fit for a MGS processing. Two gradiometer profiles to analyze are shown in Fig.5.

The first step to go into MGS processing is to convert the data code from ASCII to binary. Next a ship's heading, a ship's speed and a distance from the ship to the sensor midpoint are computed, and the sensor locations are corrected with reference to the ship's position.

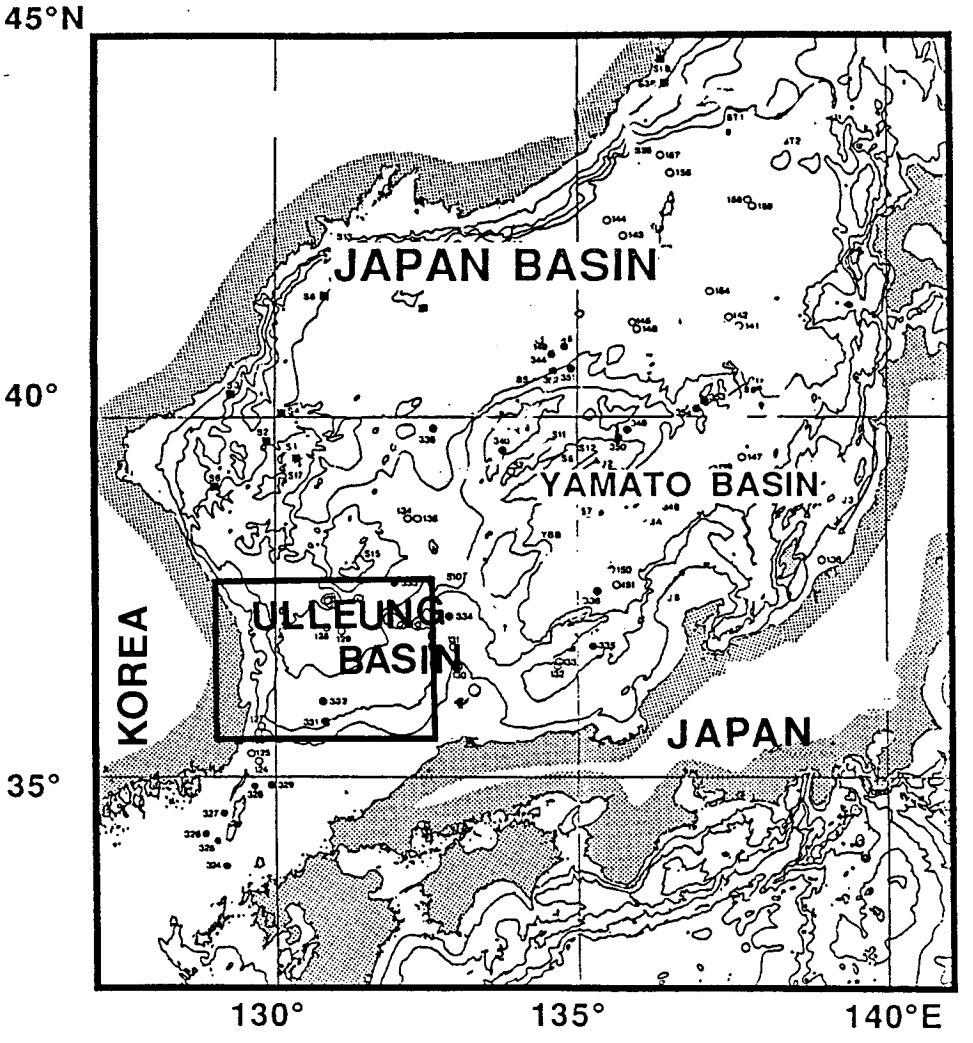

Fig. 4. The survey location

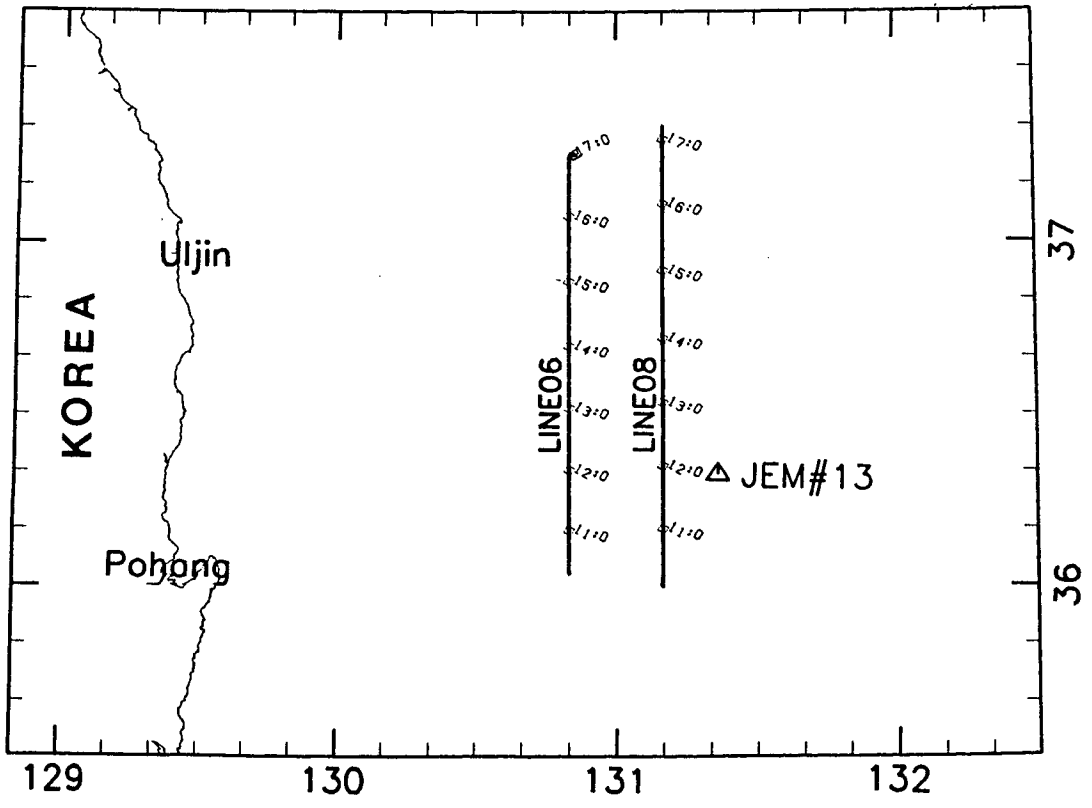

Fig. 5. Selected lines for data processing and location of OBEM station(JEM#13)

The ship's heading effects were estimated from sets of '8' pattern cruise data at three locations of the survey area. On the other hand for the lines aparted quite far from the '8' pattern cruise locations the ship's effects were eliminated using the heading coefficients calculated from several tracks with different directions.

Fig.6 shows the total magnetic profiles of two sensors along the line 06 for a sample data processing. According to sensor separation a delayed waveform can be apparently seen in the small portion selected from the whole data of the line 6(Fig.7). Lag between two sensors was determined as six for data set sampled with a interval of five seconds. Fig.8 compares slave sensor measurements with heading changes. Headings in this profile are changing with a deviation of 10 degrees from the track, which affects to slave sensor. Since generally the ship's heading remains constant along a given track, it might be expected that the heading effects would give rise to a bias between the sensor readings that would be substantially constant along each track. In such a case the heading correction could be made by removing the average difference between sensor readings to zero on each track. However since it was unfortunately known that second-order effects arising from leeway variations within tracks are amplified in integrating the gradient, the heading correction must be carefully treated to get a successful integration of the gradient.

Fig.9 shows after and before the ship's heading correction. Amount of 3 to 4 nT were adjusted from the heading correction. As a result the corrected slave sensor shows much closer match with the master sensor except for where some differences between two sensors are found as in Fig.10. Since the heading corrected slave values and master vaues were already adjusted for the ship's position and so two are different only in measured time at same position, the gaps between both sensors in parts of the profile are likely related to time varying field.

Next, amplitude spectra for the master, the slave, and the heading adjusted slave total intensities are estimated and plotted to separate time

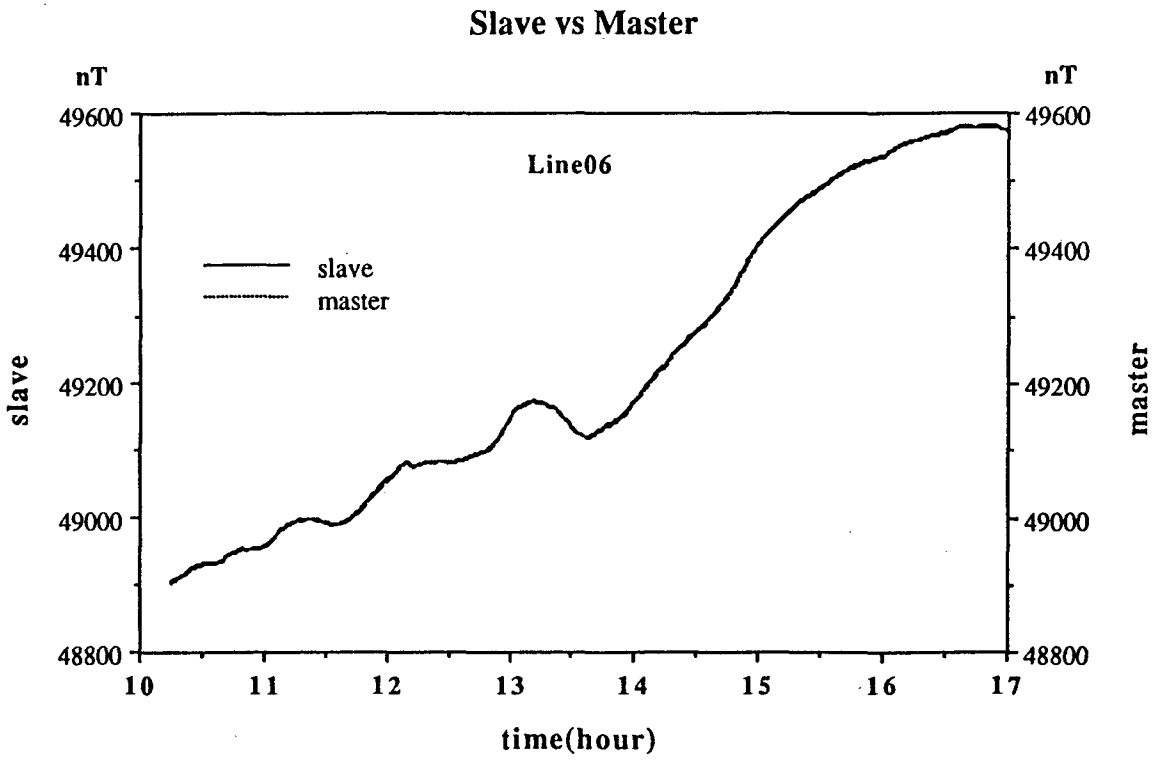

Fig. 6. Magnetic fields from the slave and the master sensor along the Line 6

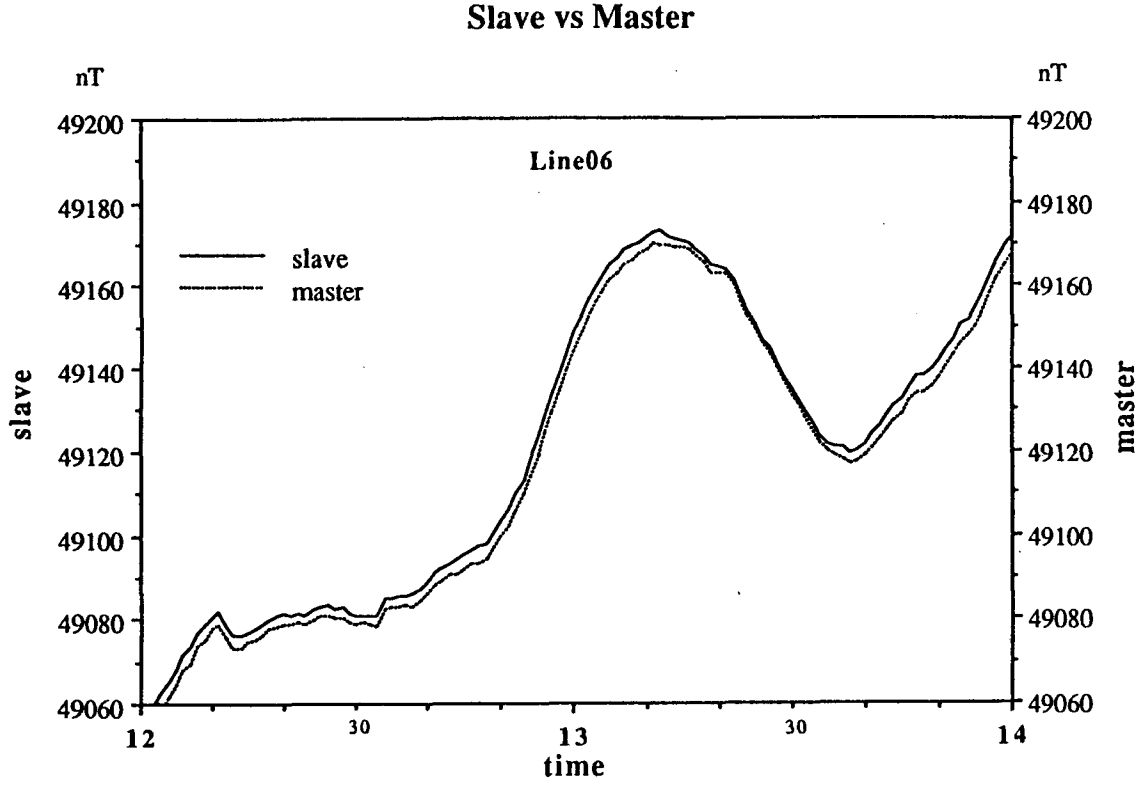

Fig. 7. Magnetic fields from the slave and the master sensor in the selected range of the Line 6.

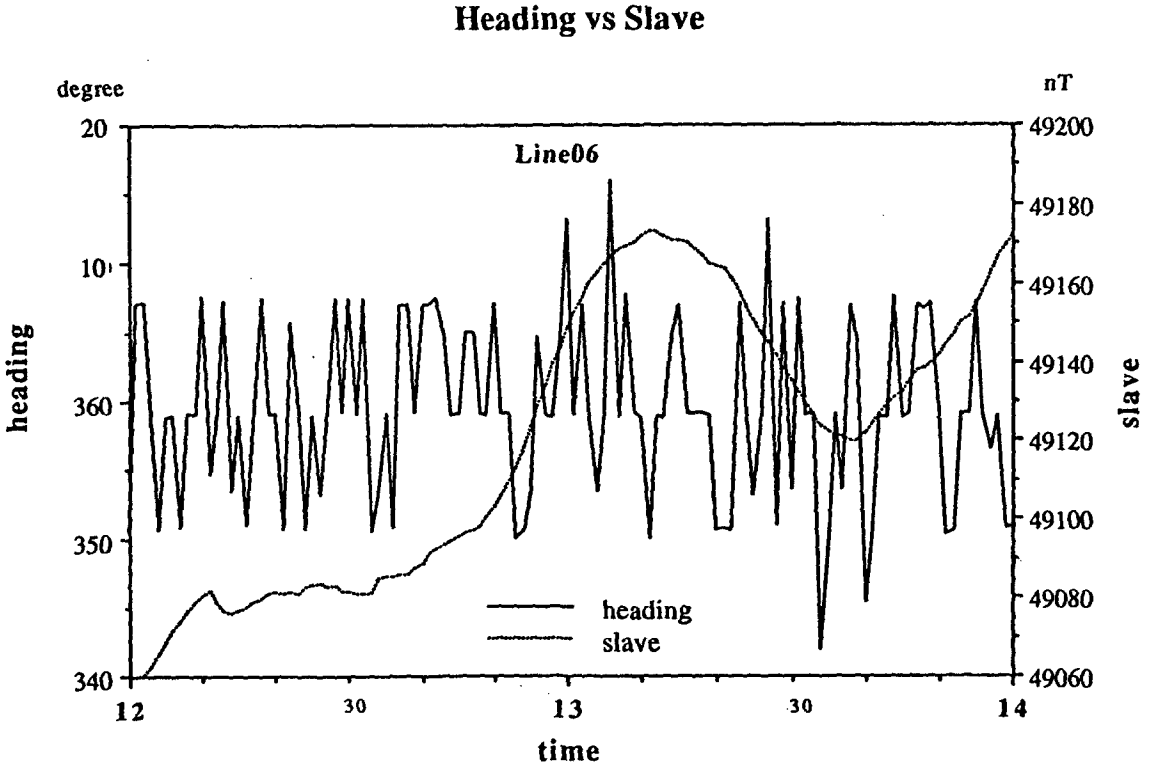

Fig. 8. Comparison of the slave sensor with the heading changes

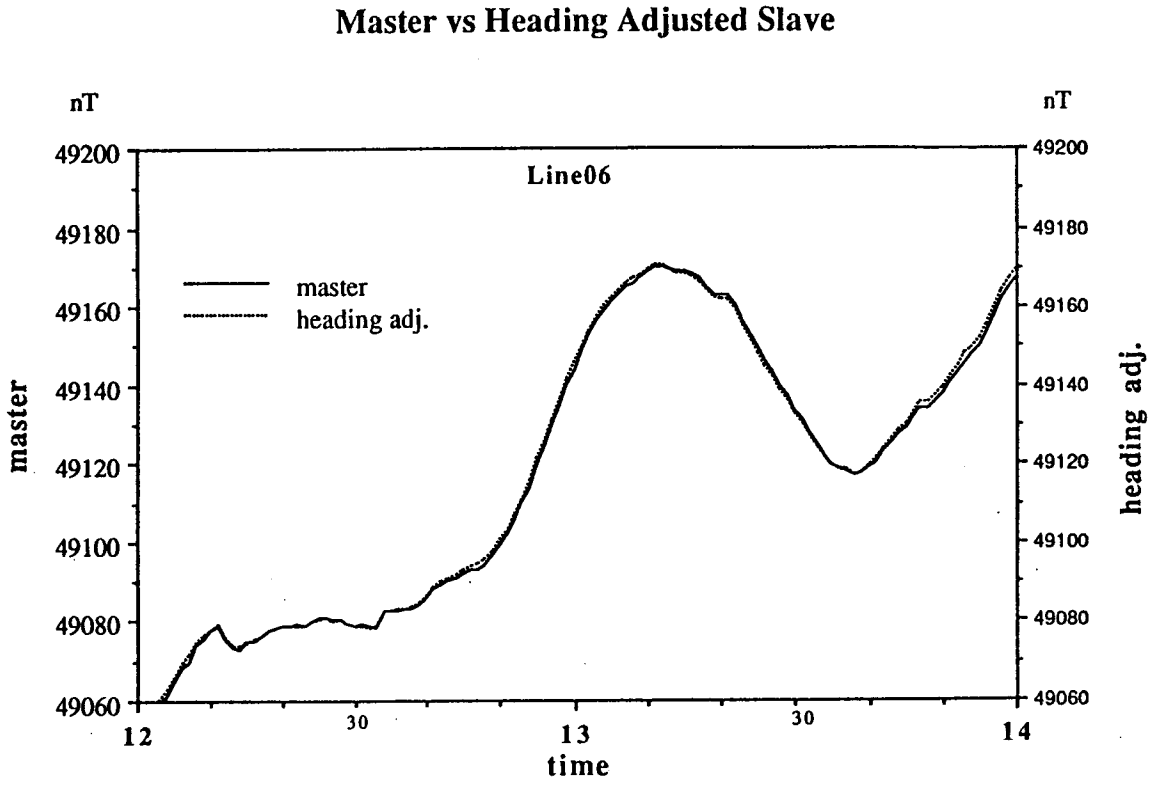

Fig. 9. Master and slave after the ship's effect is removed

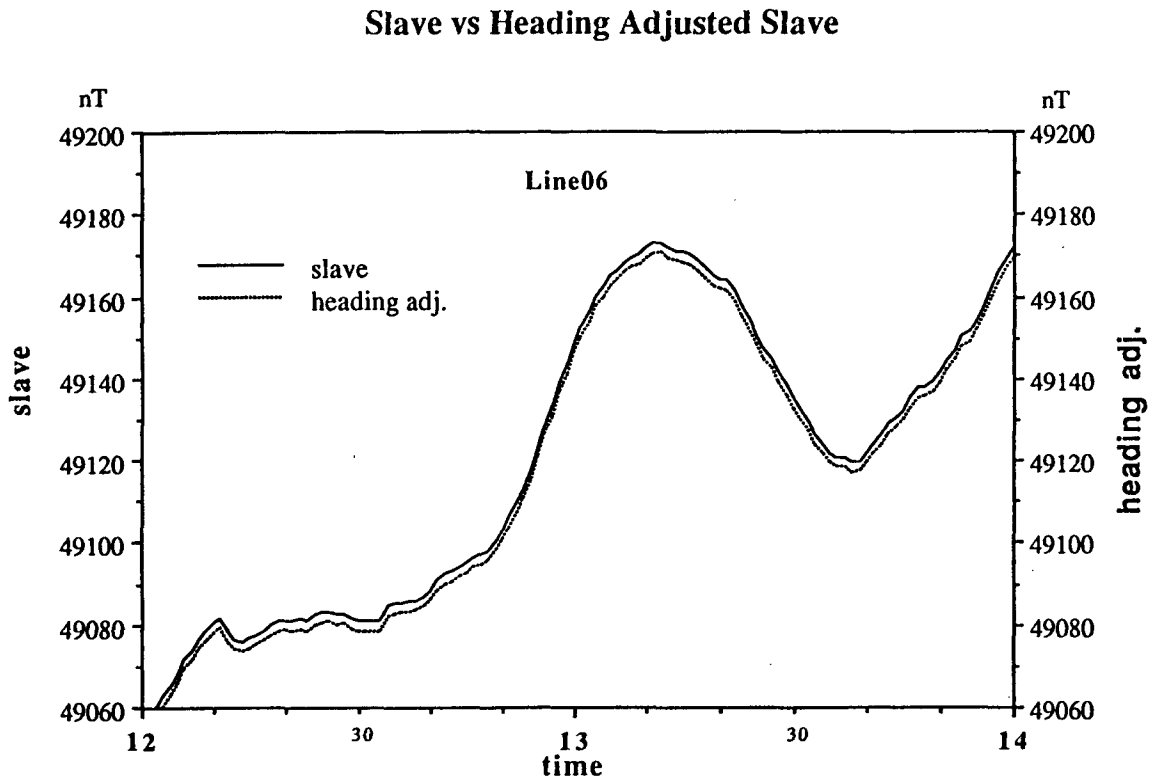

Fig. 10. Slave before and after the ship's effect is corrected

variation magnetic field from the geological signal and to reconstruct the magnetic fields free from the time variations. The spectrum calculated is the Fourier transform(Singleton, 1969) of the selected variable normalized in such a way that for white noise the average amplitude is equal to the RMS noise value(TerraSense, 1989). The frequency units are Nyquist units(cycles/sample), and all the interactions about scaling for the frequency axis is posed in these terms. Figs. 11,12,and 13 are the plot of the logarithmic amplitude spectrum to frequency for the total field from the slave sensor and the master sensor, and the heading adjusted slave sensor values, respectively, along the line 6.

Three logarithmic spectrum plots show a typical separation of a geology, time variations and a noise. The geological component is biased to low frequencies with a steep slope, while the noise dominates and appears as a nearly flat spectrum at high frequencies. Identification of the time variation may be more difficault on account of possibility to confuse it from shallow geological sources. Depth estimation method by Spector and Grant(1970) or comparisons between the slave-master difference and the derivative of the master sensor will be applied to discriminate between the geology and the time variation field. The frequency bands for the geology, the time variation and the noise are specified in the spectrum plot of Fig.13 . The staight line corresponding to the noise is appeared to be flat at high frequencies and the one for the geology is most steeply sloping at a narrow low frequency band. Whereas the time variation can be identifiable at two intermediate frequency bands with even less slopes than the geology. The natural logarithms of the intercepts of these lines with the zero-frequency axis and the slopes of the lines corresponding to the geology and the time varying signals are used to estimate reconstructed magnetic field through inverse Fourier transform.

Time varying fields estimated from the gradiometer method are compared with the time varying field measured using OBEM set up on seabottom(Fig.14). This seabottom magnetic observation was done at the area quite close to the study profiles. A dashed line in Fig.14 is a time varying magnetic profile from the OBEM observation corresponding to the same time

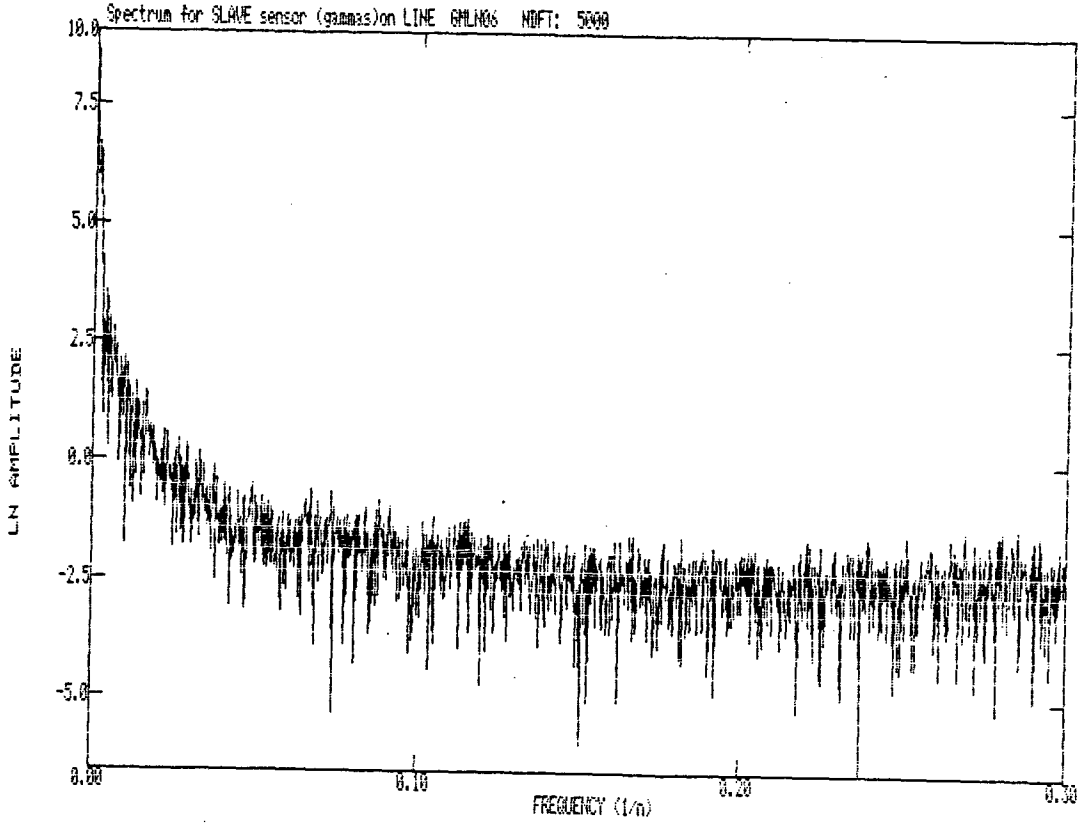

Fig. 11. Spectrum plot for slave sensor on Line 6

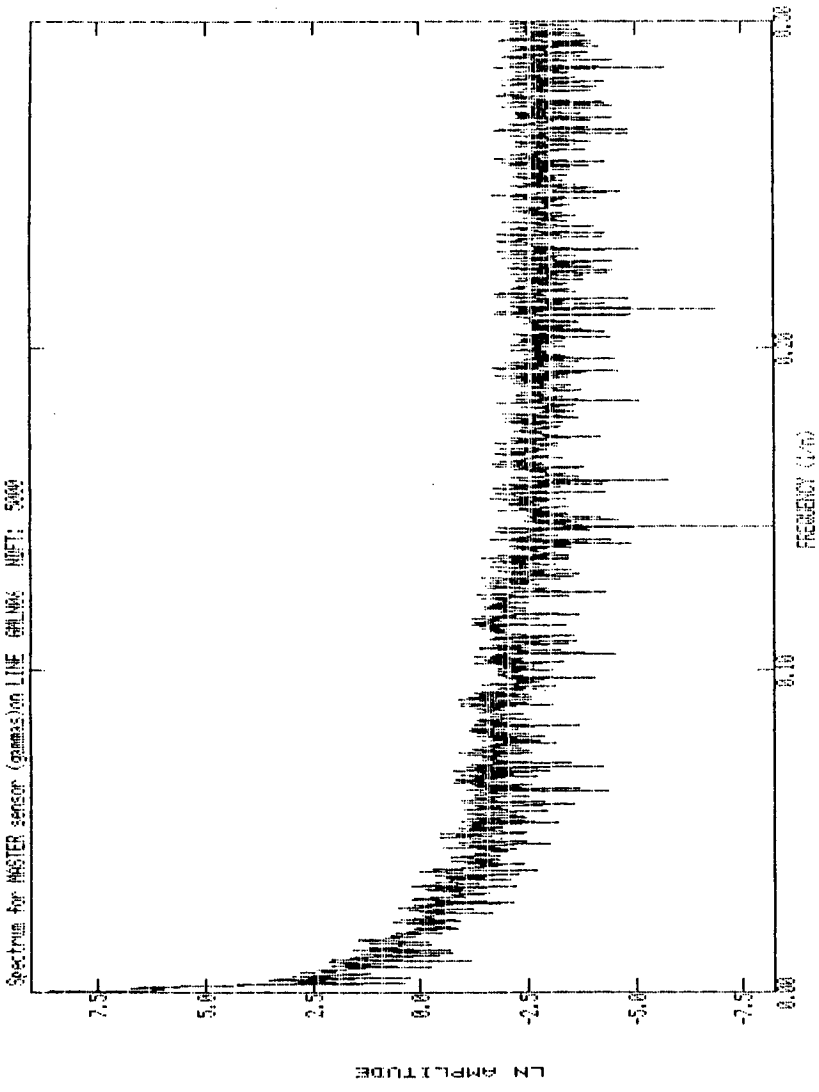

Fig. 12. Spectrum plot for master sensor on Line 6

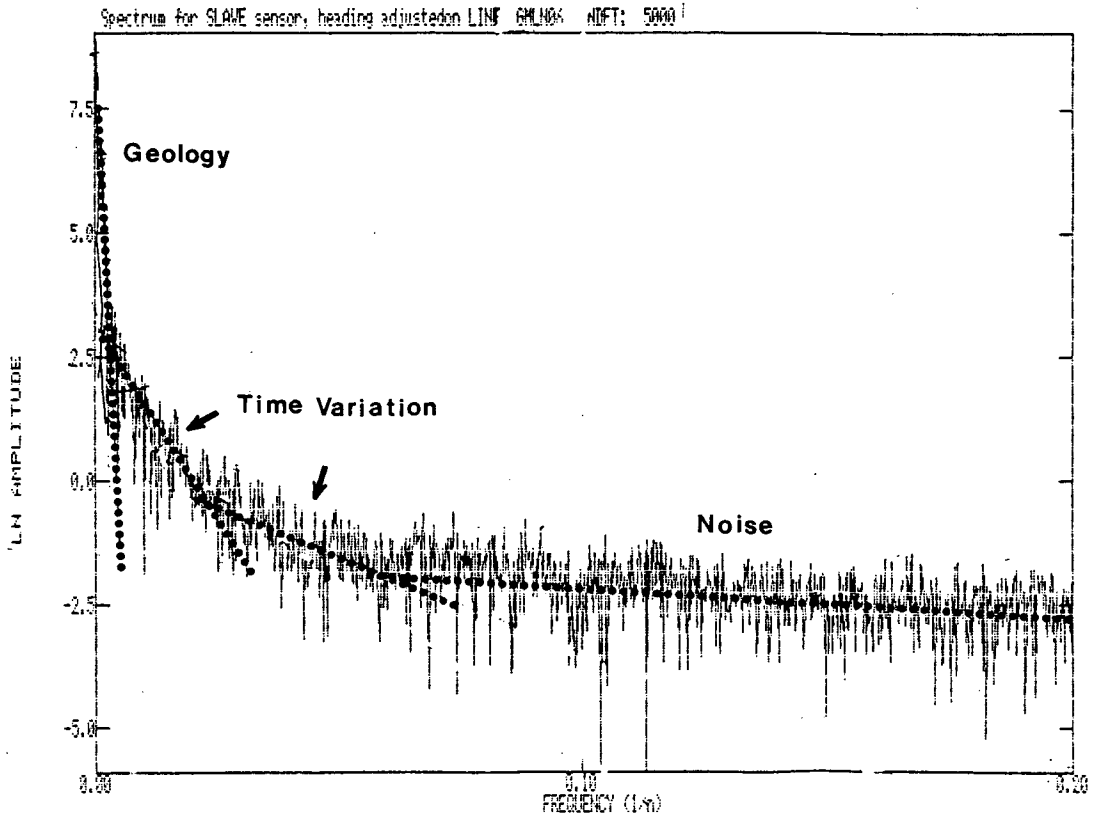

Fig. 13. Spectrum plot for heading adjusted slave sensor and determination of spectrum range for reconstruction on Line 6

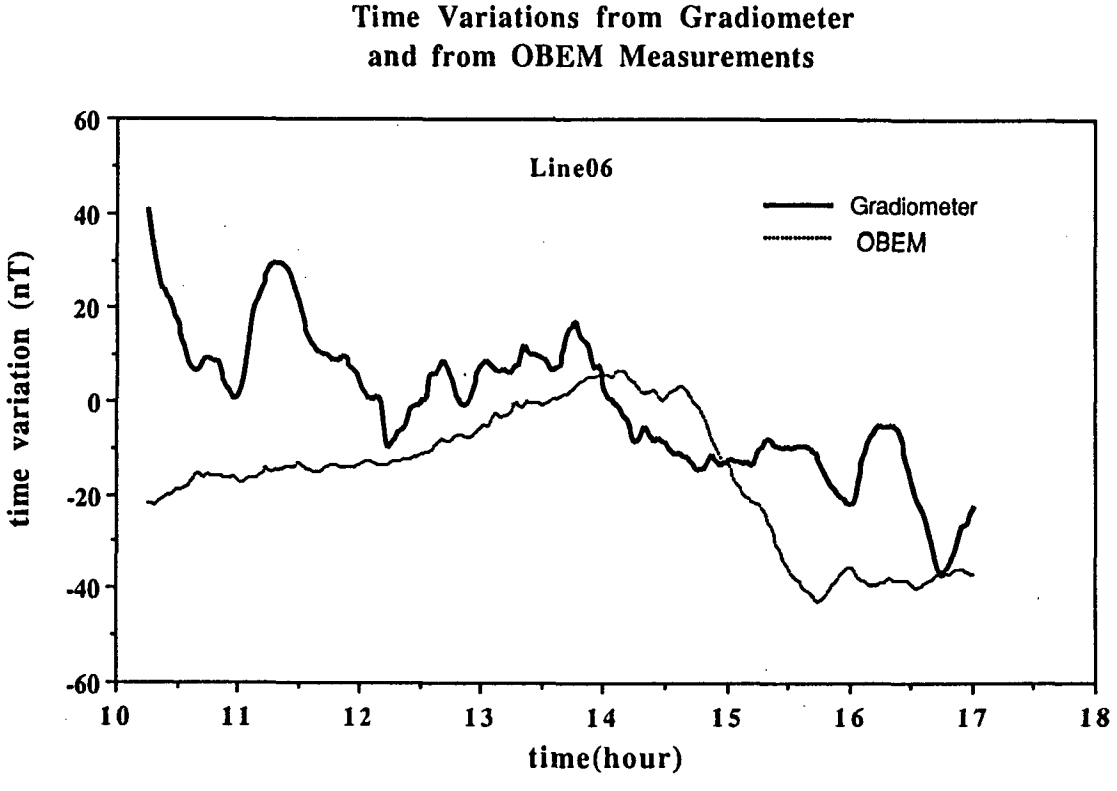

Fig. 14. Comparison of time variation from gradiometer and from OBEM measurement on Line 6

as the gradiometer profile. Two profiles shows much correlation in its shape and amplitude of most portion each other even if some minor phase shift exists and some large differences are found in amplitude between 10 to 12 o'clock.

This calculated time variations are compared with the differences between two sensor magnetic fields in Fig.15 and also with the derivatives of the master sensor magnetic field in Fig.16. The differnces between two sensors shows a similar pattern with the time vatiations indicates that the estimation of time varying field for the line 6 would be almost correct, since differences of the two magnetic fields measured at a same position with some time delay mean the time varying field.

Time varying fields at both gradiometer and OBEM appear to be considerably unstable beyond a normal behavior of geomagnetic field indicating a magnetic storm during a period of the survey. A large amount of those time variation deforms magnetic anomalies originated from geological sources to lead to an inaccurate interpretation of the magnetic data, and so it should be removed to get a correct geological interpretation.

Fig.17 compares the magnetic field from the master with the reconstructed field in which the time variation and the noise are removed. After the amount of approximately 80 nT, ranging from -40 nT to 40 nT, is corrected from the observed magnetic field, the reconstructed magnetic profile is reproduced as in Fig. 17. From the correction while the magnetic anomalies with a short wavelength become smoother, especially around end of the profile, between 10 and 12 the small anomalies are added to the longer ones so that be more complicated. Magnetic anomalies of a short wavelength at the last portion of profile could be interpreted to be attributed to time varying field than geological origin such as volcanics.

Fig.18 shows a comparison the integrated fields of derivatives with the fields reconstructed from the spectrum method. The integrated fields might fail to remove the time variation and to reconstruct the geological component. This kind of problems could often occur because several types of errors,

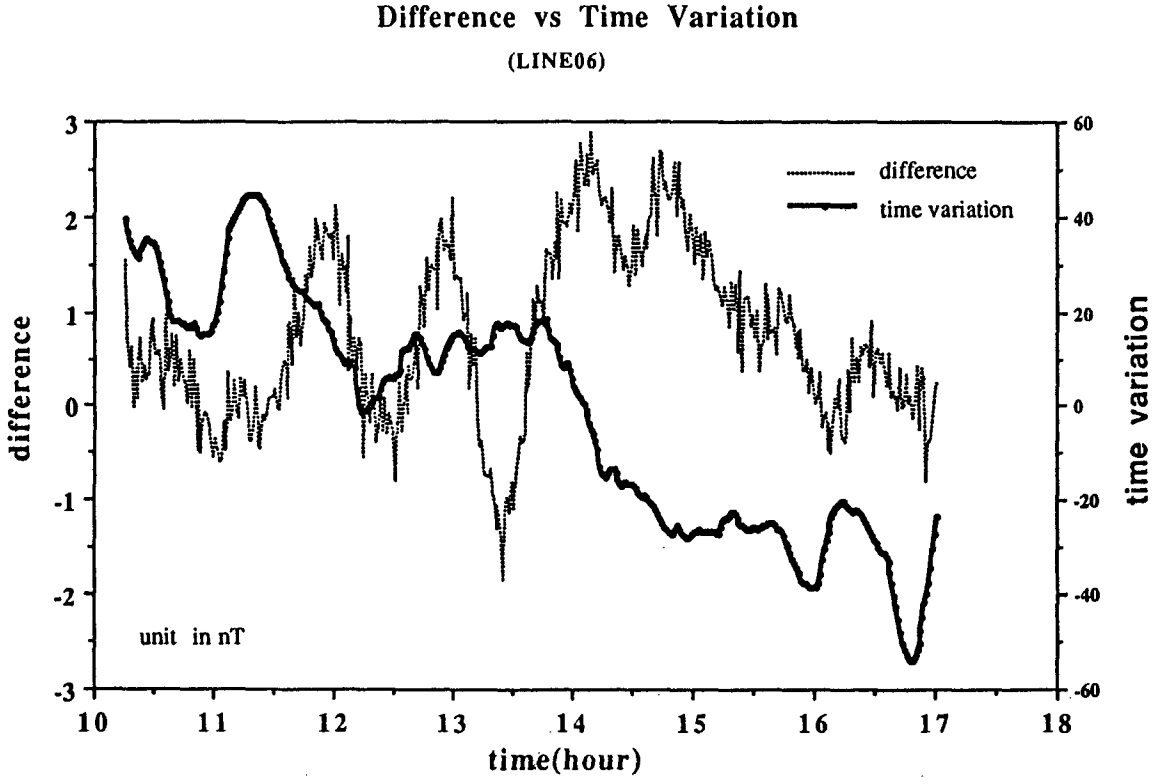

Fig. 15. Comparison of time variation and differences between two sensors on Line 6.

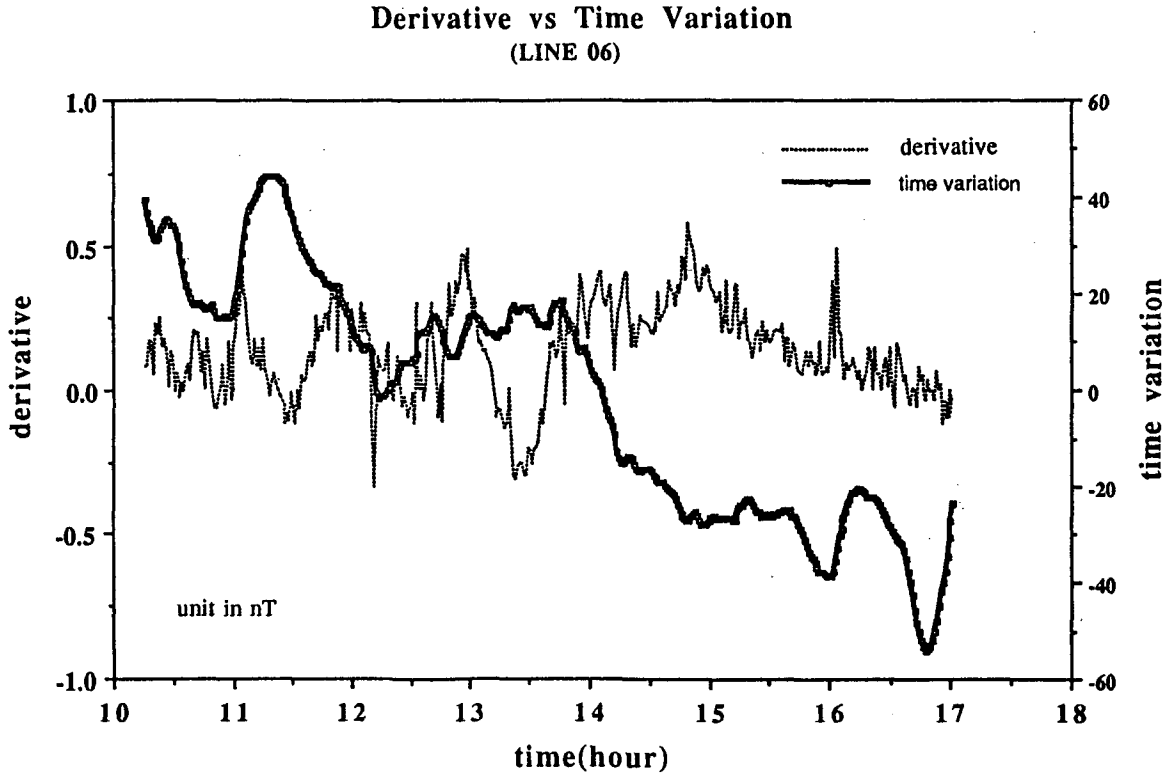

Fig. 16. Comparison of time variation and derivatives on Line 6

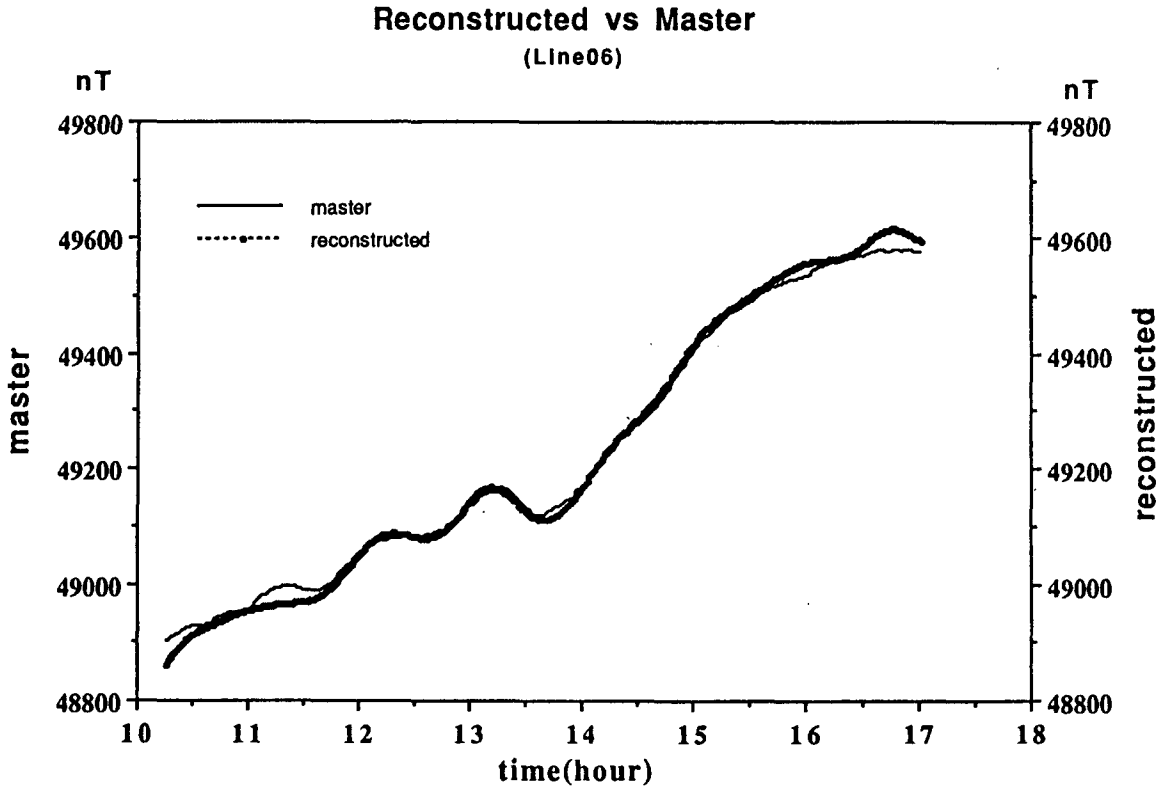

Fig. 17. Reconstructed magnetic fields free from the time variation and master fields on Line 6

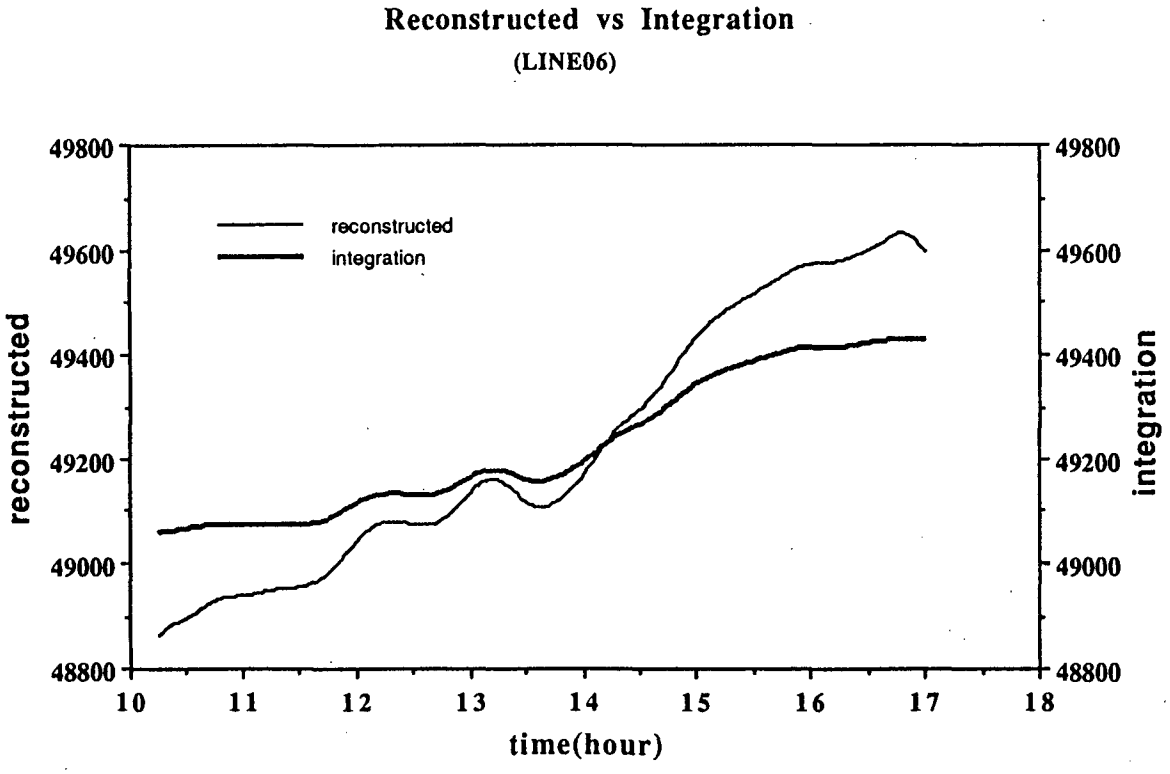

Fig. 18. Comparison of the reconstructed fields from a spectrum method and the integrated fields from derivatives on Line 6

producing relatively small effects at either sensor, are amplified in the process of estimating the gradient and re-integrating it. Consequently the numerical integration method is recommended to use as a reference of results from the reconstruction method which uses the Fourier transform of total intensities.

Fig.19 is a comparison of total intensities from the slave and master sensor along line 8. The master profile obviously shows a characteristics of less high frequency than the slave which is affected by the ship's effect and is more or less shifted relative to the slave profile by offset between both sensors. Heading effects were adjusted from the slave using the heading coefficients which are estimated from several track covering four azimuths.

Amplitude spectrum are calculated and plotted for the master, the slave, and the heading adjusted slave as shown in Figs.20,21 and 22. In these spectrum plots, three typical components for a geology, time variations and a noise are well defined as the spectrum in the line 6. The geological signals are also limited to a low frequency band, and the time variations appear in two groups of spectrums with an intermediate slope. The spectrums corresponding to the noise is appeared to be nearly flat at high frequencies. The slopes of the spectrum groups corresponding to the geology, the time varying signals and the noises are designated in Fig.22. The time variations were calculated in the reconstruction process and compared with the ones from the OBEM measurements as in Fig.23.

The computed time variations from the gradiometer data reveal more dramatical correlation to the OBEM time variations than in the line 6 on most portion of profile even with the large amplitude of anomaly around 12:40. The computed time variations as well as the OBEM time variations indicate that the earth's field were unstable with an amplitude of 40 nT ranging -10 nT to approximately 30 nT within a measured period. Once those time variations are removed, the corrected anomalies would be significantly different from the observed and represent the real effects of subsurface geology(Fig.24).

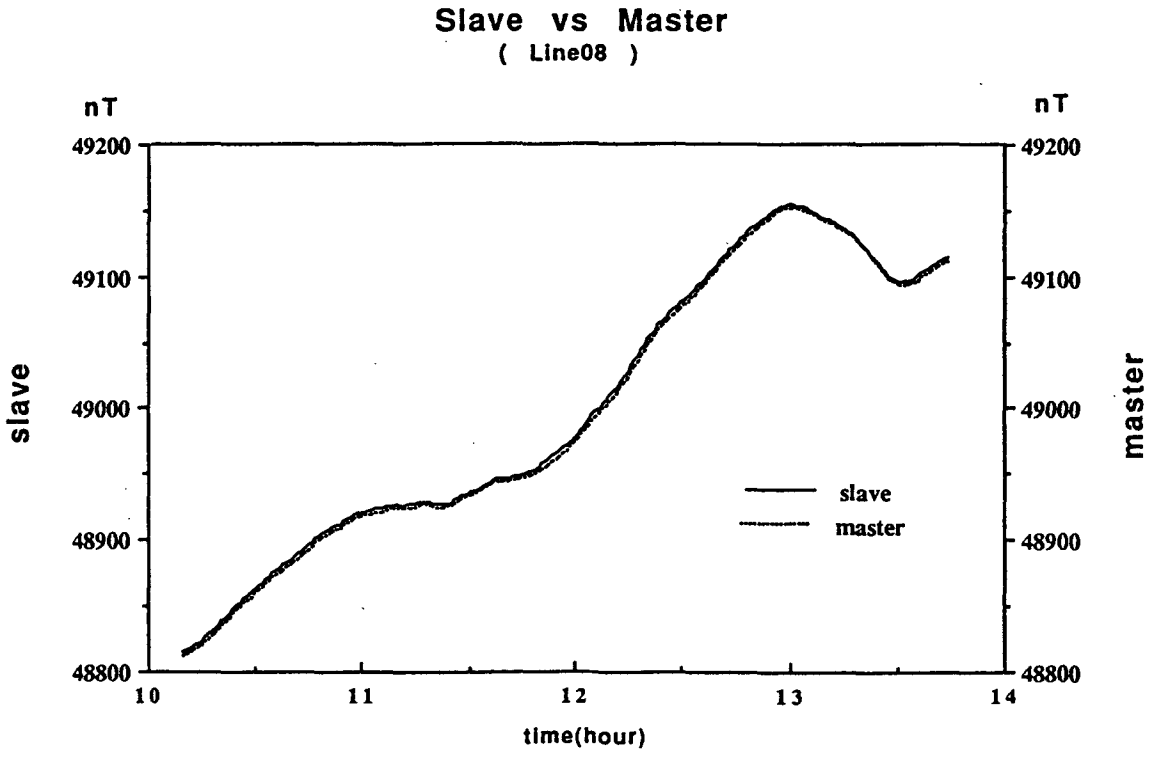

Fig. 19. Magnetic fields from the slave and the master sensor on Line 8.

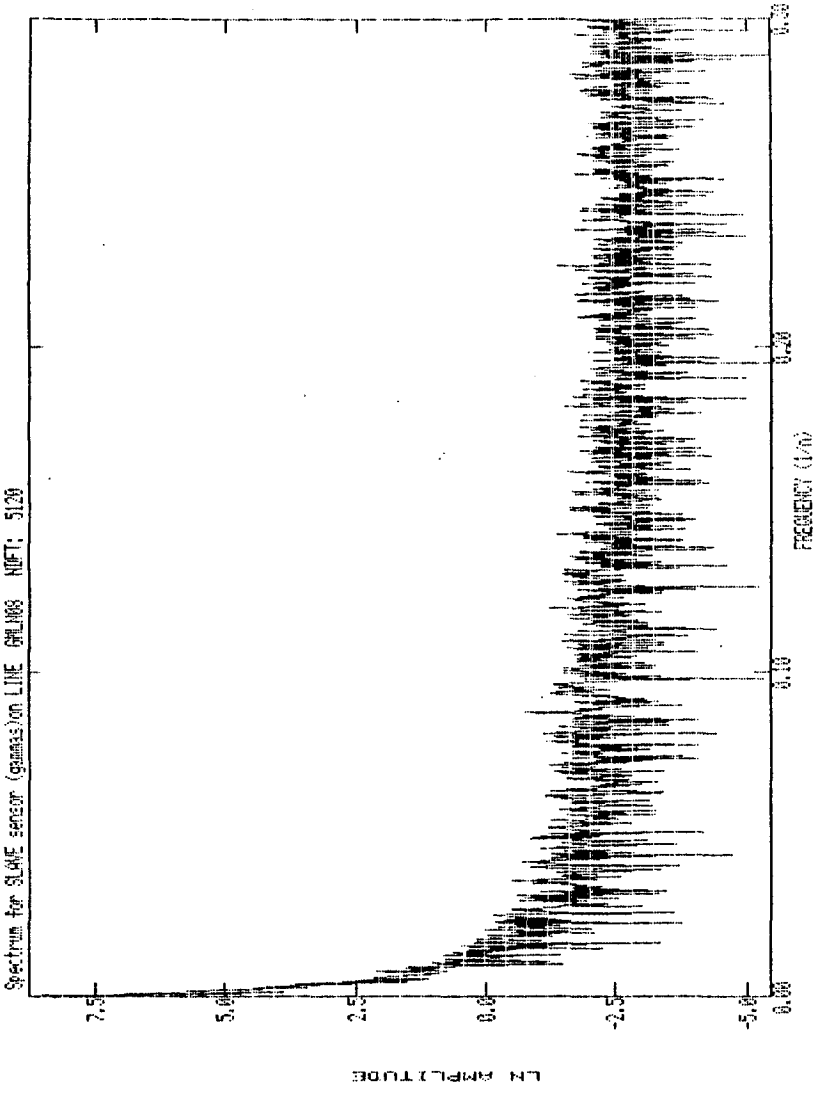

Fig. 20. Spectrum plot for slave sensor on Line 8

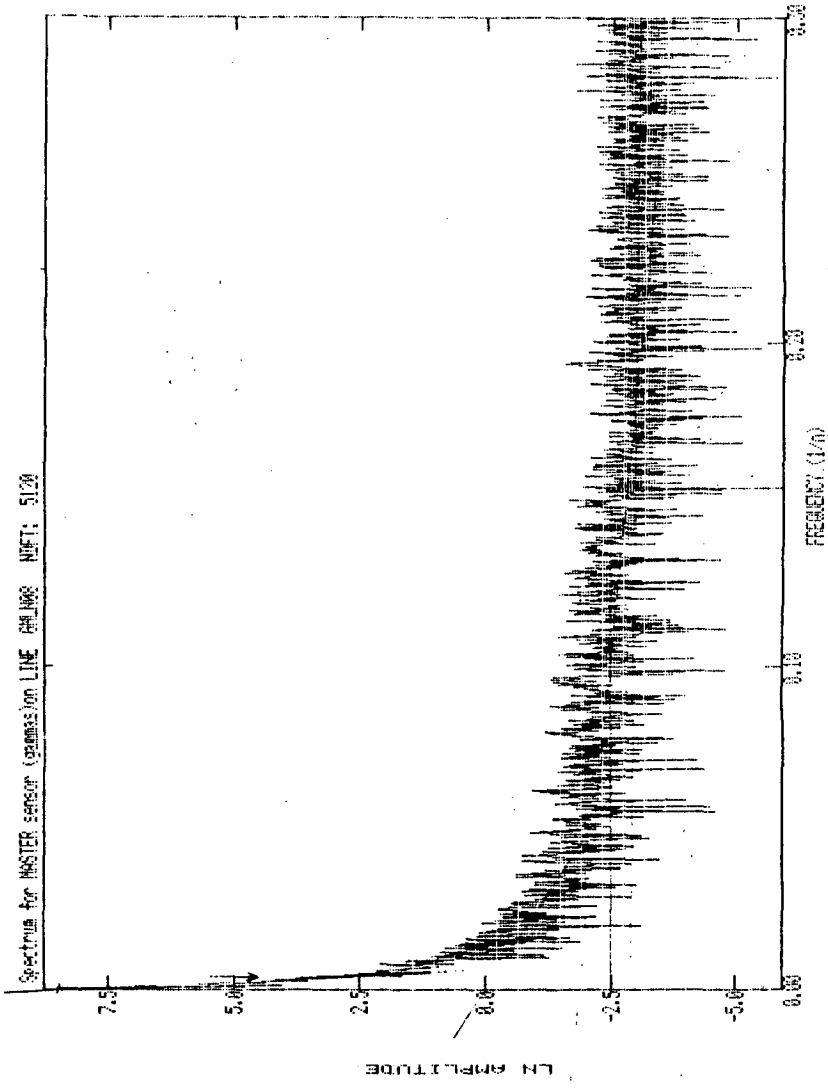

Fig. 21. Spectrum plot for master sensor on Line 8

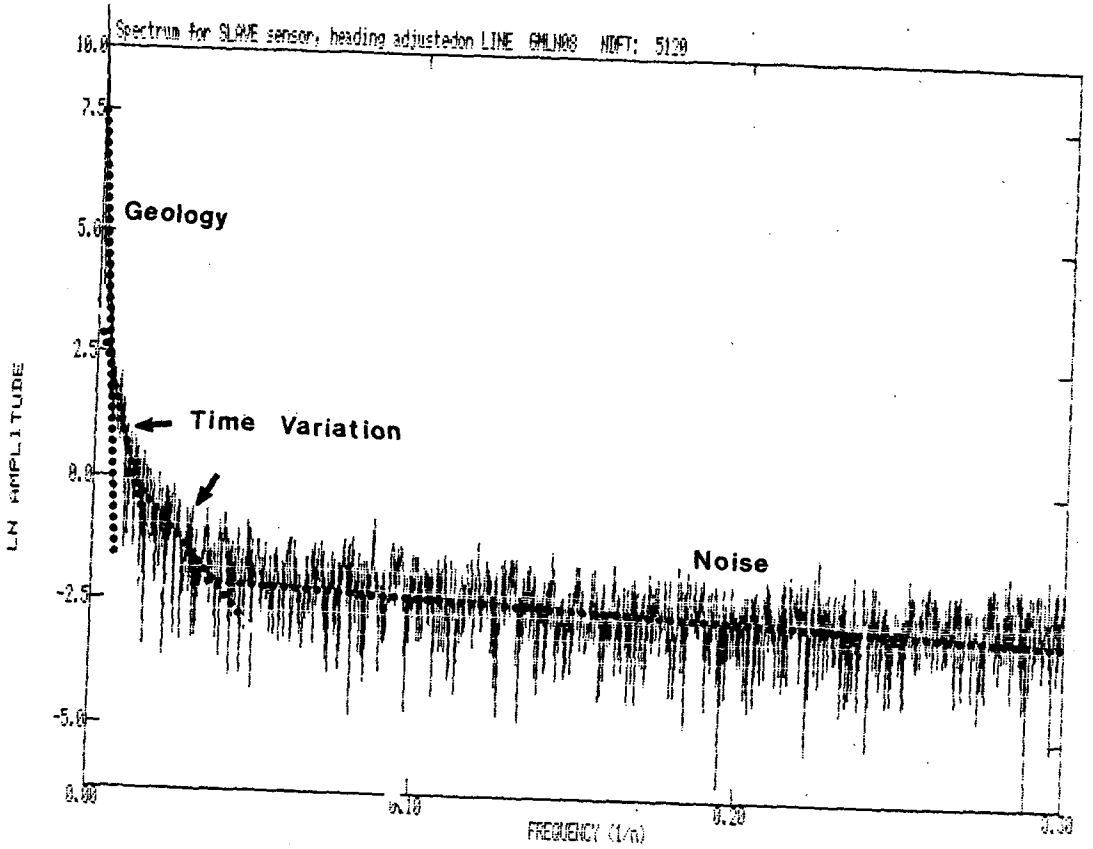

Fig. 22. Spectrum plot for heading adjusted slave sensor and determination of spectrum range for reconstruction on Line 8

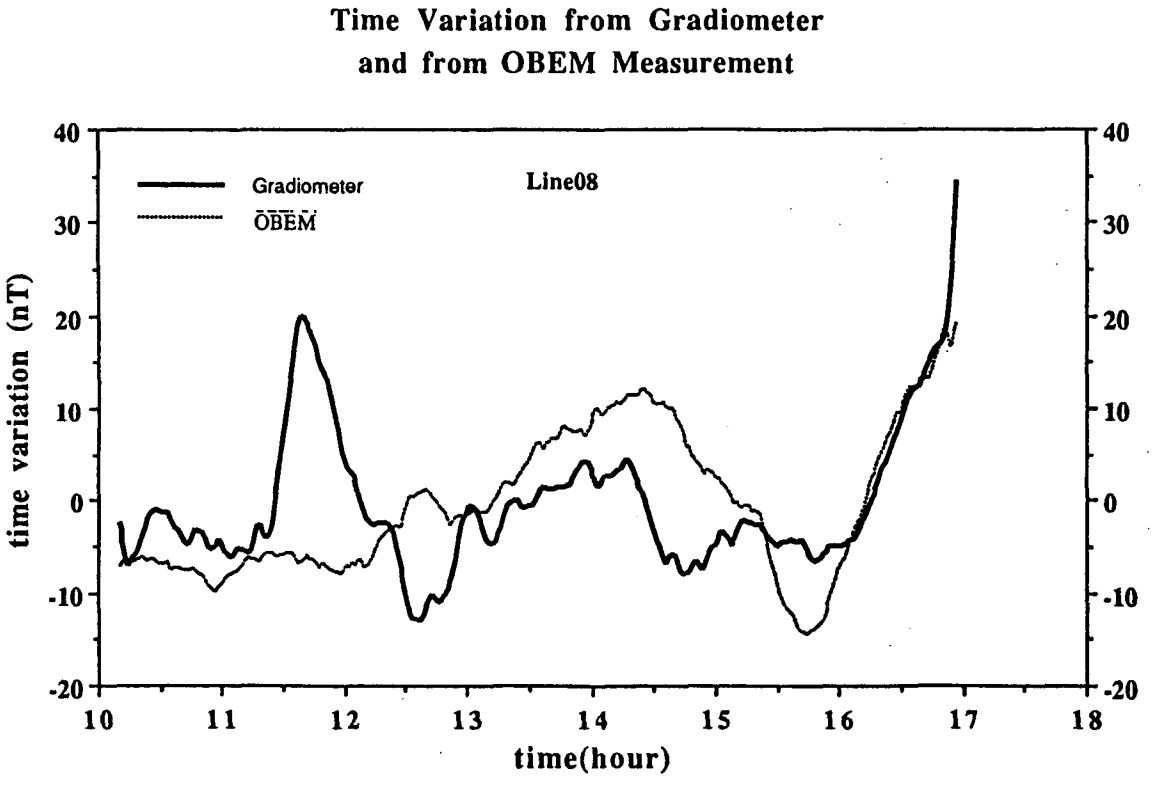

Fig. 23. Comparison of time variation from gradiometer and from OBEM measurement on Line 8

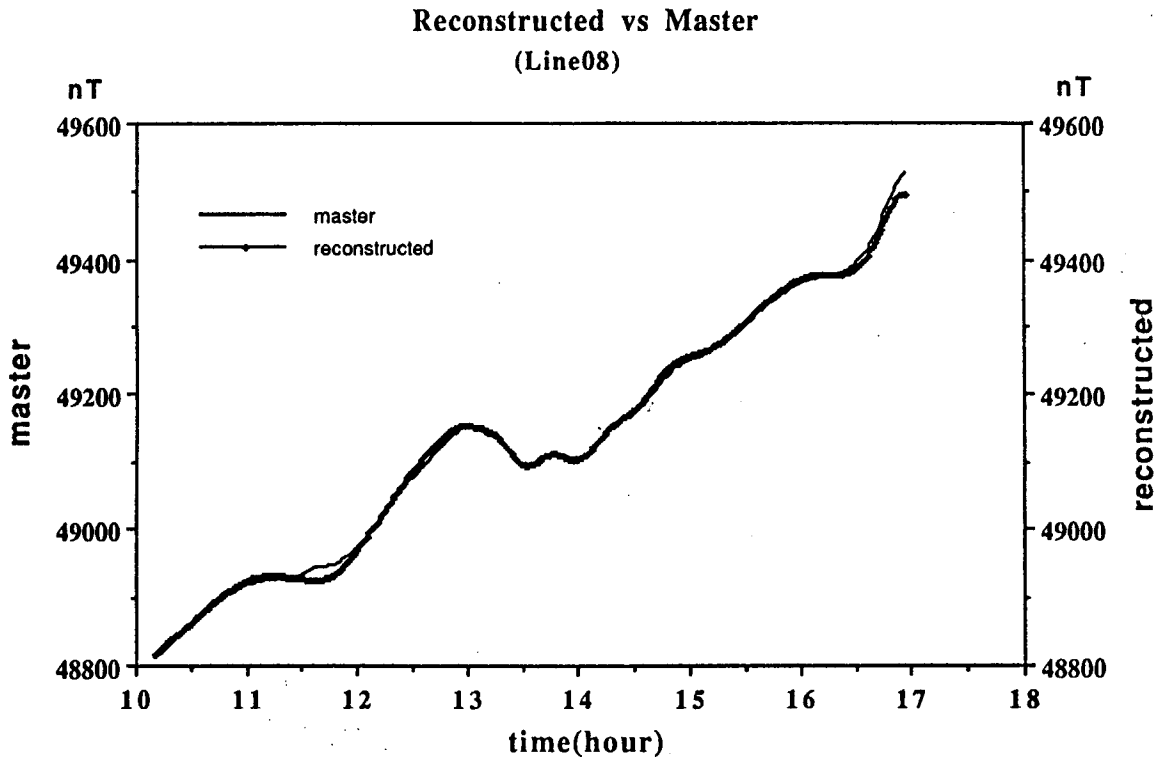

Fig. 24. Reconstructed magnetic fields free from the time variation and master fields on Line 8

CONCLUSION

In this study the first gradiometer system in Korea has been installed on the R/V Eardo, tested and completed with respect to its optimum functions, automatic digital logging system for the personal computer by obtaining real data in the Ulleung Basin area of the East Sea.

Noises or errors which could be caused by mislocation of the sensors with reference to the ship's position, the ship's magnetic properties, the instruments, the swell and sensor motion, and so on were discussed and its analysis method were applied to field gradiometer data. The ship's heading effects of 3 to 4 nT were computed from sets of '8' pattern cruise data and from the track data with more several headings and removed from the observed gradiometer data.

The magnetic fields free of the time variation from the gradiometer dat a were reconstructed from two approaches: the first is the integration of the gradient and the second is the optimum filter theory using the Fourier transform method. The reconstruction by the integration produced serious deviations, whereas the result from the optimum filter method showed an excellent correlation with the time variations of the seabottom magnetic observatory data(OBEM). Since several types of errors, creating relatively small effects at ether sensors, could be amplifed in the process of estimating the gradient and re-intergrating it, the numerical integration method is recommended to use as a reference of the results from the optimum filter method. The difference between two sensors and the gradient could be useful in descriminating the time variations from the shallow geological sources.

The time variation components of approximately 80 nT, ranging from -40 to 40 nT, was corrected from the observed magnetic data of the Line 6, and a total of about 30 nT corrected from the Line 8. These computed time variations indicate that there were some large magnetic storms in the earth's magnetic field during the survey periods.

REFERENCE

Bullard,E.C. and R.G.,Mason, 1961. The magnetic field astern of a ship, Deep-Sea Research, 8:20-27.

Hansen,R.O.,1985. Reconstruction of time variation free total fields from marine gradiometer data, EG&G Geometrics Technical Report 29.

Singleton,R.C.,1969. An algorithm for computing the mixed radix fast Fourier transform, IEEE Transactions on Audio and Electroacoustics, 17:93-103.

Spector,A. and F.S.,Grant,1970. Statistical models for interpreting aeromagnetic data, Geophys., 35:293-302.

TerraSense,Inc., 1989. Technical manual of MGScalc(Marine Gradiometer Software for PC compatible computers)

Wold,R.J. and A.K.,Cooper, 1989. Marine magnetic gradiometer-a tool for the seismic interpreter, Geophys:The leading edge of exploration.